Chemical Geology 268 (2009) 211–225

Contents lists available at ScienceDirect

Chemical Geology

journal homepage: www.elsevier.com/locate/chemgeo

Environmental analysis of paleoceanographic systems based on molybdenum–uranium covariation

T.J. Algeo [a,*], N. Tribovillard [b]

[a] Department of Geology, University of Cincinnati, Cincinnati, Ohio 45221-0013, USA
[b] Université Lille 1, Laboratoire Géosystèmes, UMR CNRS 8157, bâtiment SN5, 59655 Villeneuve d'Ascq cedex, France

ARTICLE INFO

Article history:
Received 16 May 2009
Received in revised form 29 August 2009
Accepted 2 September 2009
Editor: J.D. Blum

Keywords:
Redox
Seawater chemistry
Black Sea
Cariaco Basin
Pennsylvanian
Devonian

ABSTRACT

Modern low-oxygen marine systems exhibit patterns of molybdenum–uranium covariation that can be linked to specific attributes and processes of the depositional system, including (1) variation in benthic redox conditions, (2) the operation of particulate shuttles within the water column, and (3) the evolution of watermass chemistry. The importance of these factors in each depositional system can be assessed both from the degree of enrichment of authigenic molybdenum (Mo_{auth}) and uranium (U_{auth}) and from the $(Mo/U)_{auth}$ ratio of the sediment relative to the seawater Mo/U molar ratio of ~7.5–7.9. In open-ocean systems with suboxic bottomwaters, U_{auth} enrichment tends to exceed that of Mo_{auth} owing to onset of U_{auth} accumulation at the Fe(II)–Fe(III) redox boundary, resulting in sediment $(Mo/U)_{auth}$ ratios less than that of seawater. As bottomwaters become increasingly reducing and at least occasionally sulfidic, the rate of accumulation of Mo_{auth} increases relative to that of U_{auth}, and sediment $(Mo/U)_{auth}$ ratios equal or exceed that of seawater. In restricted marine systems with permanently sulfidic deepwaters, the relative enrichment of Mo_{auth} and U_{auth} depends on additional factors. In the Cariaco Basin, which has an aqueous Mo/U ratio similar to that of seawater, the operation of a particulate Mn–Fe-oxyhydroxide shuttle serves to accelerate the transfer of Mo to the seafloor, leading to strong enrichments in Mo_{auth} relative to U_{auth}. In the Black Sea, the chemistry of the deep watermass has evolved to the point where its aqueous Mo/U ratio is only ~0.04 that of seawater, as a consequence of which sediments deposited under deepwater influence are depleted in Mo_{auth} relative to U_{auth}. These Mo–U covariation patterns can be used to gain a better understanding of the watermass attributes and processes of ancient low-oxygen marine systems. Analysis of anoxic facies from two North American paleomarine systems, the Late Pennsylvanian Midcontinent Sea (LPMS) and the Late Devonian Seaway (LDS), reveals authigenic Mo–U relationships similar to those of the modern marine environments above, implying similar redox and hydrographic controls. The observed patterns are consistent with laterally unconfined circulation and strong watermass exchange within the LPMS, and with markedly restricted deepwater circulation in silled basins of the LDS. Patterns of authigenic Mo–U covariation may prove useful in analysis of other paleoceanographic systems to reveal aspects of watermass composition and environmental dynamics.

1. Introduction

1.1. Analysis of paleoceanographic systems

Reconstruction of environmental conditions and processes within ancient marine systems requires the use of multiple proxies, including trace-metal concentration data. Trace-metal concentrations have long been used to draw inferences concerning paleoredox conditions (Brumsack, 1980; Wignall and Myers, 1988; Dean et al., 1999; Tribovillard et al., 2006), in which samples are generally classified as oxic (>2.0 ml O_2 L^{-1}), dysoxic or suboxic (~0.2–2.0 ml O_2 L^{-1}), anoxic–nonsulfidic (<0.2 ml O_2 L^{-1}, 0 ml H_2S L^{-1}), and anoxic–sulfidic or euxinic (0 ml O_2 L^{-1}, >0 ml H_2S L^{-1}) (Savrda and Bottjer, 1991; Wignall, 1994). In addition, recent studies have shown that trace-metal concentration data can provide information concerning a wider range of paleoenvironmental parameters, including the chemical evolution of watermasses, deepwater residence times, and the degree of restriction of silled anoxic basins (Algeo and Lyons, 2006; Algeo et al., 2007; Algeo and Maynard, 2008).

The present study aims to build on this earlier work by examining patterns of covariation between Mo and U in modern and ancient anoxic marine systems. Mo and U are particularly useful for paleoenvironmental analyses because of several characteristics (Table 1). Both elements are present in low concentrations in the upper continental crust (average 2.7 ppm for U, 3.7 ppm for Mo; Taylor and McLennan, 1985). Both elements exhibit conservative behavior under

---

[*] Corresponding author. Tel.: +1 513 556 4195.
E-mail address: Thomas.Algeo@uc.edu (T.J. Algeo).

0009-2541/$ – see front matter © 2009 Elsevier B.V. All rights reserved.
doi:10.1016/j.chemgeo.2009.09.001

Table 1
Characteristics of molybdenum and uranium.

Characteristic	Molybdenum	Uranium
Biologically essential element	Yes	No
Ocean distribution	Conservative	Conservative; a small but variable fraction of is associated with particulate organic carbon
Salinity-normalized dissolved concentration	110 nM	13 nM
Modern-ocean residence time	0.78 million years	0.45 million years
Main source of metal	Rivers	Rivers
Main species in oxic sea water and oxidation state	MoO_4^{2-}/Mo(VI)	$UO_2(CO_3)_3^{4-}$/(U(VI))
Speciation in reducing conditions	Thiomolybdates $MoO_xS_{4-x}^{2-}$	UO_2, U_3O_7 or U_3O_8
Main mechanisms of transfer to sediments	In oxic settings, Mo scavenging by metal oxides, notably Mn (probable speciation change from the dissolved MoO_4^{2-} to the particle reactive MoO_3). In reducing settings with free HS^-, Mo is converted to particle reactive thiomolybdates that are scavenged from solution *via* sulfidized (organic S-rich) organic material r *via* Mo capture by Fe–S phases. At low [HS^-], Mo uptake probably occurs in the presence of Fe, possibly mediated by a Fe—S phase. At high sulfide concentrations, uptake must operate in the absence of dissolved iron possibly mediated by a metal sulfide such as MoS_4^{2-}.	The main removal mechanism operates via uptake across the sediment-water interface of reducing sediments. Under conditions close to the Fe(III)–Fe(II) transition, soluble U (VI) is reduced to insoluble U(IV), the uptake of which may be accelerated by the formation of organometallic ligands and the influence of organic substrates in the sediment. The accumulation is at least partly mediated by bacterial sulfate reduction reactions, because without bacterial activity, the reduction process is slow. As sulfate reduction intensity is linked to reactive organic matter abundance, U concentration is usually correlated with the organic carbon rain rate and content in anoxic (non-sulfidic) facies.

oxic conditions and have long residence times in seawater (~450 kyr for U, ~780 kyr for Mo). Consequently, both elements exhibit nearly uniform concentrations in seawater globally, yielding a seawater Mo/U molar ratio of 7.53 ± 0.25 in the Pacific Ocean (Chen et al., 1986; Millero, 1996) and 7.90 ± 0.30 in the Atlantic Ocean (Morris, 1975; Chen et al., 1986). Additionally, both elements are present in low concentrations in plankton, so enrichments in sediments or sedimentary rocks generally can be imputed to authigenic uptake of these elements from seawater. For both elements, such uptake is greatly facilitated by oxygen-depleted conditions. Notwithstanding these similarities, there are important differences in the behavior of Mo and U under reducing conditions that can lead to differences in their abundances in marine sediments: (1) U_{auth} uptake commences at the Fe(II)–Fe(III) redox boundary (Zheng et al., 2002a,b), earlier than Mo_{auth} uptake, which requires the presence of H_2S (Helz et al., 1996; Zheng et al., 2000); and (2) transfer of Mo_{auth} to the sediment can be accelerated through a particulate Mn–Fe-oxyhydroxide shuttle (Murray, 1975; Crusius et al., 1996), whereas U_{auth} is unaffected by this process. Given these differences in behavior, an analysis of patterns of authigenic Mo–U covariation has the potential to provide useful, as-yet-unrecognized insights concerning environmental conditions and processes in paleoceanographic systems. As shown below, authigenic Mo–U covariation can yield information concerning (1) variation in benthic redox conditions, (2) the operation of particulate shuttles within the water column, and (3) the evolution of watermass chemistry. Our approach is first to analyze authigenic Mo–U covariation in modern low-oxygen marine systems to gain an understanding of the range of observed patterns and their environmental significance, and then to apply these findings to an analysis of authigenic Mo–U covariation in black shales of the Late Pennsylvanian Midcontinent Sea (LPMS) and the Late Devonian Seaway (LDS) of the North American craton.

1.2. Molybdenum and uranium behavior in aqueous systems

The mechanisms of uptake of authigenic Mo by sediments are now fairly well understood. Under oxic conditions, Mo is present in seawater as the stable and largely unreactive molybdate oxyanion (MoO_4^{2-}). Mo_{auth} enrichment is limited in oxic environments, and modern continent-margin sediments typically contain only 1–5 ppm (Zheng et al., 2000; Morford et al., 2009a). Under anoxic–sulfidic conditions, Mo becomes "activated" at a critical activity of hydrogen sulfide ($a_{HS^-} = 10^{-3.6}$ to $10^{-4.3}$, equivalent to ~50–250 µM HS^-), which facilitates conversion of molybdate (MoO_4^{2-}) to thiomolybdates ($MoO_xS_{(4-x)}^{2-}$, $x = 0$ to 3) (Helz et al., 1996; Zheng et al., 2000). In the latter form, Mo is particle reactive and readily adsorbed onto humic substances or Mn- and Fe-oxyhydroxides (Berrang and Grill, 1974; Magyar et al., 1993; Helz et al., 1996; Tribovillard et al., 2004). Although uptake of Mo by particulates can occur within the water column, as shown by sediment trap data (Berrang and Grill, 1974; François, 1988), most Mo uptake probably occurs at or just below the sediment/water interface (François, 1988; Emerson and Huested, 1991; Crusius et al., 1996; Zheng et al., 2000; Morford et al., 2009a). The relatively greater importance of uptake by the sediment may be due to the much longer residence time of particles on the seafloor than in the water column, or possibly due to the higher sulfide concentrations encountered below the sediment/water interface (Meyers et al., 2005). Other factors that may favor Mo uptake at or below the sediment/water interface include the presence of Brønsted acids in porewaters, which promote the molybdate-to-thiomolybdate conversion, and the availability of clay mineral surfaces, which may catalyze hydrolysis and sulfidation of thiomolybdates (Erickson and Helz, 2000; Vorlicek and Helz, 2002).

Mn–Fe redox cycling represents an important additional mechanism of authigenic Mo enrichment in some marine systems (Berrang and Grill, 1974; Jacobs et al., 1985; Emerson and Huested, 1991; Magyar et al., 1993; Crusius et al., 1996; Morford et al., 2005). Particulate Mn–Fe-oxyhydroxides form at the chemocline and adsorb molybdate oxyanions during transit through the water column. Upon reaching the sediment/water interface, these particles are reductively dissolved, releasing molybdate ions that then either diffuse back into the water column or are scavenged by other phases within the sediment (Morford and Emerson, 1999; Morford et al., 2005). The latter process accelerates the transfer of Mo_{auth} to the sediment relative to other redox-sensitive trace metals (e.g., U) that do not participate in this particulate shuttle, leading to elevated $(Mo/U)_{auth}$ ratios. The importance of Mn–Fe redox cycling for authigenic Mo accumulation is dependent on the vertical position of the chemocline. Such redox cycling has little influence on Mo_{auth} accumulation where the chemocline is located (1) within the sediment, as in oxic–suboxic facies, or (2) high within a stably stratified anoxic water column, as in the Black Sea or Framvaren Fjord, where molybdate is reductively released back into the water column (Jacobs et al., 1985; Skei et al., 1996; Crusius et al., 1996). In contrast, in environments with suboxic to weakly sulfidic deepwaters, especially those subject to redox variations at short timescales, Mn–Fe redox cycling may be a major factor in enhancing Mo transfer to the sediment (Murray, 1975; Crusius et al., 1996). In such settings, vertical fluctuations of the chemocline alternately promote (1) Mo scavenging in the water column when the chemocline recedes below the sediment/water interface and oxidizing (albeit suboxic) deepwaters catalyze precipitation of solid-phase Mn–Fe-oxyhydroxides, and (2) Mo release at the sediment/water interface when the chemocline rises into the water column and sulfidic bottomwaters catalyze reductive dissolution of Mn–Fe-oxyhydroxides in surficial sediments. This process represents a "Mo pump" that may be responsible for the exceptionally large Mo_{auth} burial fluxes in marine systems such as the Cariaco Basin and Saanich Inlet (Algeo and Lyons, 2006, their figure 7A).

The aqueous geochemistry of U exhibits some important similarities and differences to that of Mo. Under oxic–suboxic conditions, U is present mainly as soluble U(VI) in the form of uranyl carbonate complexes $(UO_2(CO_3)_3^{4-})$ that are chemically unreactive (Langmuir, 1978; Klinkhammer and Palmer, 1991; Calvert and Pedersen, 1993). U_{auth} enrichment is limited in oxic environments, and modern continent-margin sediments typically contain only 1–5 ppm (Morford et al., 2009b). Under anoxic conditions, U(VI) is reduced to U(IV), forming the highly soluble uranyl ion UO_2^+ or less soluble uranous fluoride complexes. Reduction of U(VI) does not seem to occur within the water column but, rather, only within the sediment (Anderson et al., 1989; McManus et al., 2005), suggesting that the reduction process may take place on particle surfaces, possibly catalyzed by enzymes produced by iron and sulfate-reducing bacteria (Barnes and Cochran, 1990; Zheng et al., 2002a; Morford et al., 2009a). In the reduced state, uptake of U_{auth} by sediments may occur through: (1) formation of organic-metal ligands in humic acids, or (2) precipitation of crystalline uraninite (UO_2) or a metastable precursor to it (Klinkhammer and Palmer, 1991; Zheng et al., 2002a). U reduction commences at the Fe(II)–Fe(III) redox boundary and may be controlled by microbially-mediated Fe redox reactions rather than by the presence of HS^- (Zheng et al., 2002a). Thus, the onset of U_{auth} enrichment occurs under less intensely reducing conditions and at shallower depths within the sediment column than that of Mo_{auth} (Morford et al., 2009a). U is not known to be influenced by Mn–Fe redox cycling in the water column, a difference in behavior that can potentially result in markedly different levels of enrichment of U_{auth} and Mo_{auth} in marine sediments.

The accumulation of both U_{auth} and Mo_{auth} is influenced by exposure to oxic porewaters. Authigenic Mo and U adsorbed onto particulates are released through oxidative remineralization of the solid phase, a process which occurs mainly close to the sediment-water interface and which can lead to a large diffusive flux of Mo and U out of the sediment (Morford et al., 2009a). In oxic marine systems, this process is strongly promoted by biotic irrigation (bioturbation) of the sediment (Zheng et al., 2002b; Morford et al., 2009b). Under such conditions, only a fraction (~20 to 70%) of Mo and U delivered to the sediment is ultimately retained in authigenic phases (Morford et al., 2009a,b). Sediment porewater data provide no evidence for post-depositional remobilization of Mo and U in anoxic facies, where the diffusive flux of Mo and U across the sediment-water interface is nearly equal to their rates of authigenic accumulation (Morford et al., 2009a). However, oxygenation of organic- and trace-metal-rich sediments can lead to remobilization of authigenic Mo and U, resulting in either loss to the overlying water column or vertical redistribution within the sediment (Thomson et al., 1995, 1998; McManus et al., 2005). Vertical migration of redox-sensitive trace metals over distances of a few cm to a few dm commonly results in concentration peaks at redox interfaces within the sediment (Colley and Thomson, 1985; Thomson et al., 1995, 1998). Post-depositional redistribution of Mo and U has the potential to alter the primary depositional concentrations and concentration ratios of these metals, although existing studies provide no evidence to suggest any systematic difference in their remobilization potential.

1.3. Molybdenum and uranium enrichment factors

To compare the respective enrichments of Mo_{auth} and U_{auth} in the study formations, trace-metal concentrations are given in the form of "enrichment factors" (EF), where $X_{EF} = [(X/Al)_{sample}/(X/Al)_{PAAS}]$, and X and Al stand for the weight concentrations of element X and Al, respectively. Samples were normalized using the post-Archean average shale (PAAS) compositions of Taylor and McLennan (1985). Although Al normalization has some potential pitfalls (Van der Weijden, 2002; Tribovillard et al., 2006), enrichment factors are useful for rapid assessment of the authigenic fraction of Mo and U in large numbers of samples. In practice, a detectable authigenic enrichment corresponds to $X_{EF} > 3$ and a substantial enrichment to $X_{EF} > 10$. For all the depositional systems examined here, sample data are shown in the form of Mo_{EF}–U_{EF} crossplots, in which the seawater Mo/U molar ratio is also shown as a guide to interpreting *relative* enrichments of Mo_{auth} versus U_{auth}. Although contemporaneous seawater Mo/U molar ratios are unknown for Pennsylvanian and Devonian sediments, it seems unlikely that seawater [Mo] and [U] have varied much through time in view of their long residence times in seawater (~780 and 450 kyr, respectively).

2. Mo–U covariation in modern marine systems

The present analysis focuses on three low-oxygen modern marine environments representing different types of depositional systems. The eastern tropical Pacific is a continent-margin upwelling system in which low-oxygen conditions are primarily due to high productivity but also influenced by deepwater restriction within silled depressions such as the California Borderland basins. The Cariaco Basin represents a moderately restricted anoxic silled basin of normal-marine salinity with moderate levels of primary productivity, whereas the Black Sea represents a strongly restricted anoxic silled basin of brackish salinity with low levels of primary productivity. Differences in the physicochemical conditions of these three depositional systems and in the processes operating within them are inferred to account for differences in their authigenic Mo–U covariation patterns.

2.1. Background

2.1.1. Eastern tropical Pacific

Strong upwelling along the North American and South American continental margins results in elevated levels of primary productivity, organic carbon sinking fluxes, and benthic oxygen utilization (McManus et al., 2006). Oxygen deficient conditions are generally prevalent along the continental slopes at depths of 500–1500 m (the oxygen minimum zone, or OMZ; Fig. 1A) but also extend onto the continental shelves at depths of <200 m at ~5–22°N and ~3–12°S latitude (Levitus and Boyer, 1994; Algeo et al., 2008). Locally in the southern California Borderland region and on portions of the Mexican Margin and Peru Shelf, tectonic subsidence has produced silled basins within which deepwater exchange is reduced and dissolved oxygen levels are further depleted relative to adjacent shelf areas (Fig. 1A; Berelson et al., 1987; Berelson, 1991; Berelson et al., 1996; Zheng et al., 2000; McManus et al., 2006). Variability in dissolved oxygen levels is more limited within these restricted basins, in which $[O_2]$ is consistently <0.5 ml L^{-1} (<20 μM) than for unrestricted continental slope settings (Fig. 2).

The southern California Borderland region consists of a series of basins and swells, in which many of the former accumulate at least intermittently laminated sediments under anoxic conditions (Berelson et al., 1987, 1996; Shaw et al., 1990; Berelson, 1991; McManus et al., 2005). Dissolved oxygen concentrations are lower throughout the water columns of the basins, where benthic redox conditions are commonly suboxic, than in adjacent shelf areas (Fig. 1A). In the past few years, the areal extent of suboxic conditions in the California Borderland region has expanded, especially at water depths shallower than 100 m (Chan et al., 2008). Average bulk sediment (92 g cm^{-2} kyr^{-1}) and organic

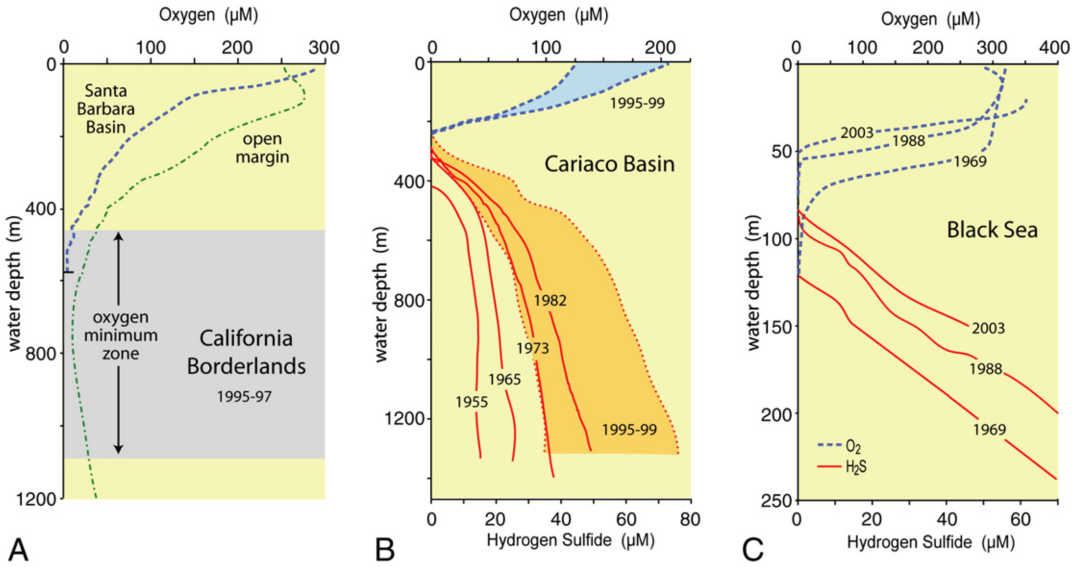

Fig. 1. Redox profiles for modern low-oxygen systems: (A) California Borderlands, (B) Cariaco Basin, and (C) Black Sea. Concentrations of dissolved oxygen (blue) and hydrogen sulfide (red) are plotted versus depth. In A, shading shows depth range of the oxygen minimum zone. In B, gray shading shows ranges of O_2 and H_2S values for the years 1995–1999. Data sources: (A) Zheng et al. (2002b); (B) Scranton et al. (2001) and Ho et al. (2004); (C) Murray et al. (1989; 1991) and Knorr 2003 expedition database (www.ocean.washington.edu/cruises/Knorr2003/index.html). (For interpretation of the references to colour in this figure legend, the reader is referred to the web version of this article.)

carbon (2.8 g cm^{-2} kyr^{-1}) accumulation rates range from high in the Santa Barbara Basin (Thunell et al., 1995; Kennett and Ingram, 1995) to moderate (10-30 g cm^{-2} kyr^{-1} and 0.5-2 g cm^{-2} kyr^{-1}, respectively) in other basins (McManus et al., 2005). The Central California shelf exhibits less bathymetric variation but is also subject to generally high although temporally variable rates of upwelling and primary productivity (Gardner and Hemphill-Haley, 1986; Dean et al., 1997).

The Mexican Margin exhibits a strong oxygen-minimum zone at depths of ~100–800 m (Wyrtki, 1967; Dean et al., 2006). The Soledad site, west of Baja California, and the San Blas site, in the Gulf of California, are located within restricted continental slope basins: the Soledad Basin is 545 m deep with a sill depth of 250 m, and the San Blas Basin is 430 m deep with a sill depth of 300 m. Mazatlan is an unbroken continental slope setting within the Gulf of California (Nameroff et al., 2002). These sites are all characterized by low benthic dissolved oxygen concentrations (<0.5 μM; Fig. 2; van Geen et al., 2003; Berelson et al., 2005), although bulk sediment (~5–10 g cm^{-2} kyr^{-1}) and organic carbon (~0.5–1.0 g cm^{-2} kyr^{-1}) accumulation rates are generally lower than in the California Borderland basins (van Geen et al., 2003; Dean et al., 2006).

The Peru Margin is characterized by high productivity as a consequence of wind-driven upwelling, especially during La Nina events within the ~4–7-yr-long ENSO cycle (Suits and Arthur, 2000). As a consequence, redox conditions are generally anoxic and locally sulfidic at water depths from 75 to 550 m, and sediments have TOC values to ~20% and highly enriched trace-metal concentrations (Reimers and Suess, 1983; Böning et al., 2004). The Mo–U data from the Peru Margin in McManus et al. (2006) is from a depth of 264 m within the Pisco Basin, a small tectonic depression characterized by very high organic carbon accumulation rates (~30 g cm^{-2} kyr^{-1}) and a local minimum in dissolved oxygen levels (<0.5 μM; Fig. 2; Zuta and Guillén, 1970; Zuta et al., 1978).

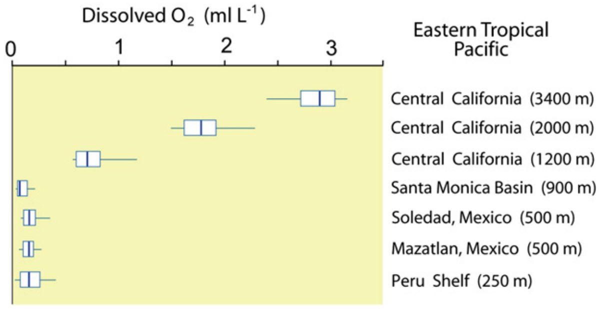

Fig. 2. Redox variability in low-oxygen environments of the eastern tropical Pacific. Each bar-and-whisker plot shows the median (thick vertical line), 16th and 84th percentile values (bar), and minimum and maximum values (thin horizontal line) for a time series of dissolved oxygen observations in each area.

Data sources: CalCOFI 1949–2007 database (www.calcofi.org/) and Zuta et al. (1978). For comparison with Fig. 1, 3.0 ml/L O_2 is approximately equal to ~130 μM oxygen.

Aqueous Mo and U concentration profiles for the eastern tropical Pacific are similar to those for seawater globally and show little vertical variation (Fig. 3A; Bruland, 1983; Chen et al., 1986). Although profiles for most of the specific sites at which sediment samples were collected are unavailable (but see Nameroff et al., 2002), aqueous trace-metal concentrations are unlikely to vary much in the eastern tropical Pacific owing to generally uninhibited watermass exchange (Wyrtki, 1967). Some restriction of the deep watermasses in the silled basins of the California Borderland region occurs, possibly influencing watermass chemistry to a limited degree. Aqueous Mo/U molar ratios for the eastern tropical Pacific are uniformly between 7.0 and 8.0.

The sediment Mo and U concentration data for the eastern tropical Pacific (Fig. 4A) were taken from McManus et al. (2006), who reported Mo–U concentration data for three sites on the central California margin (1455 to 3595 m), six sites within the southern California Borderland region (896 to 3707 m), three sites on the Mexico Margin (430 to 542 m), and one site on the Peru Shelf (264 m). These data were supplemented with Mo–U data from ODP Site 1017, which was located at a water depth of 955 m on the continental slope to the west of Point Conception on the southern California margin (Tada et al., 2000; Irino et al., 2000). These samples were taken from the upper 5.6 m of a 24.9-m-long piston core, representing calcareous silt and clay interspersed with normally graded sand layers of probable turbiditic origin that was deposited from ~25 kyr B.P. to the present (Kennett et al., 2000). TOC ranges from 0.5 to 3% (average 1.6%) and the sediment is almost completely bioturbated, reflecting mainly oxic to suboxic benthic redox conditions.

2.1.2. Cariaco and Orca basins

The Cariaco Basin, the second-largest anoxic silled basin in the modern world, is a ~7000-km^2 tectonic depression on the Venezuelan continental shelf (Jacobs et al., 1987). It consists of two >1400-m-

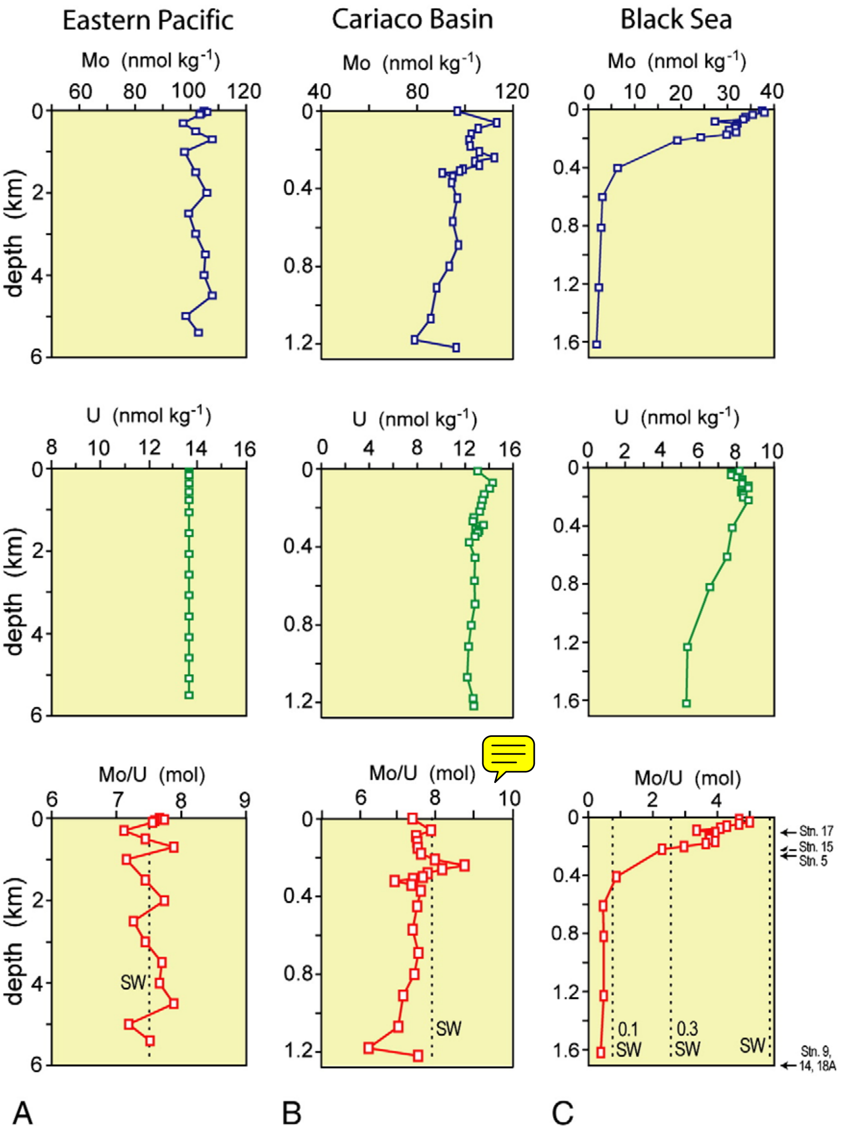

Fig. 3. Aqueous profiles of Mo, U, and Mo/U molar ratio for modern marine systems: (A) eastern tropical Pacific, (B) Cariaco Basin, and (C) Black Sea. Dotted lines show the seawater (SW) Mo/U ratio (~7.5 in the Pacific region and ~7.9 in the Atlantic region) in all Mo/U plots and fractions thereof for the Black Sea.
Data sources: (A) Bruland (1983) and Chen et al. (1986); cf. Nameroff et al. (2002); (B) Anderson (1987) and Emerson and Huested (1991); (C) Anderson et al. (1989) and Emerson and Huested (1991).

deep subbasins separated by a ~900-m-deep saddle and is bordered by shallow sills (~120–150 m) that limit deepwater exchange. The watermass is of marine salinity, and water-column stratification is maintained by a thermocline. The renewal time (τ_{dw}) of the deep watermass is ~50–100 yr (Algeo and Lyons, 2006). The O_2/H_2S interface has shallowed from ~400 m to ~200 m water depth since the 1950s (Fig. 1B; Jacobs, 1984; Jacobs et al., 1987; Scranton et al., 1987; Zhang and Millero, 1993; Scranton et al., 2001; Ho et al., 2004). Below the chemocline, $[H_2S]_{aq}$ increases downward to a maximum value of ~30–80 µM at the sediment/water interface, although substantial interannual variation has been observed (Scranton et al., 2001; Ho et al., 2004). Overspills of denser masses of oxygenated water that descend to depths of ~200–500 m are frequent (Scranton et al., 2001; Astor et al., 2003). Anoxia was established ~14.5 kyr B.P. when the deglacial eustatic rise brought nutrient-rich Caribbean intermediate waters into the basin, stimulating primary productivity and increasing deepwater oxygen demand (Peterson et al., 1991; Haug et al., 1998; Werne et al., 2000; Lyons et al., 2003). At present, seasonal shifts in the Intertropical Convergence Zone (ITCZ) and in trade wind strength result in intensified upwelling between January and May, triggering elevated primary production and vertical fluxes of organic carbon (Müller-Karger et al., 2001). Organic carbon accumulation rates average 1–6 g cm^{-2} kyr^{-1} and the sedimentary organic matter is mostly of marine origin (Dean et al., 1999; Thunell et al., 2000; Müller-Karger et al., 2001; Lyons et al., 2003). In addition to photosynthesis in surface waters, carbon also is fixed by chemoautotrophic activity at high rates (0.1 to 3.3 times surface productivity) at and just below the O_2/H_2S interface (Taylor et al., 2001).

The Orca Basin is a small (~400 km^2), deep (~2400 m) depression on the continental slope of the northern Gulf of Mexico (Shokes et al., 1977; Sheu, 1990; Hurtgen et al., 1999; Tribovillard et al., 2008). The depression is bordered by sills at ~2000 m, resulting in a shallow (<200-m-thick) restricted deep watermass. The contact between the bulk of the watermass, which is of "normal" seawater chemistry, and the restricted deep watermass occurs over a ~50-m-thick transition zone below ~2200 m. Across this contact, salinity increases from 35 ppt to ~260 ppt, density jumps from 27 to 180 (σ_t), dissolved oxygen falls to zero, and hydrogen sulfide rises transiently to >3 µM (peaking at ~2250 m before falling to zero in the deepest part of the water column. The exceptionally strong pycnocline severely limits exchange between the restricted deep watermass and the overlying water column. The basin formed as a consequence of salt tectonics

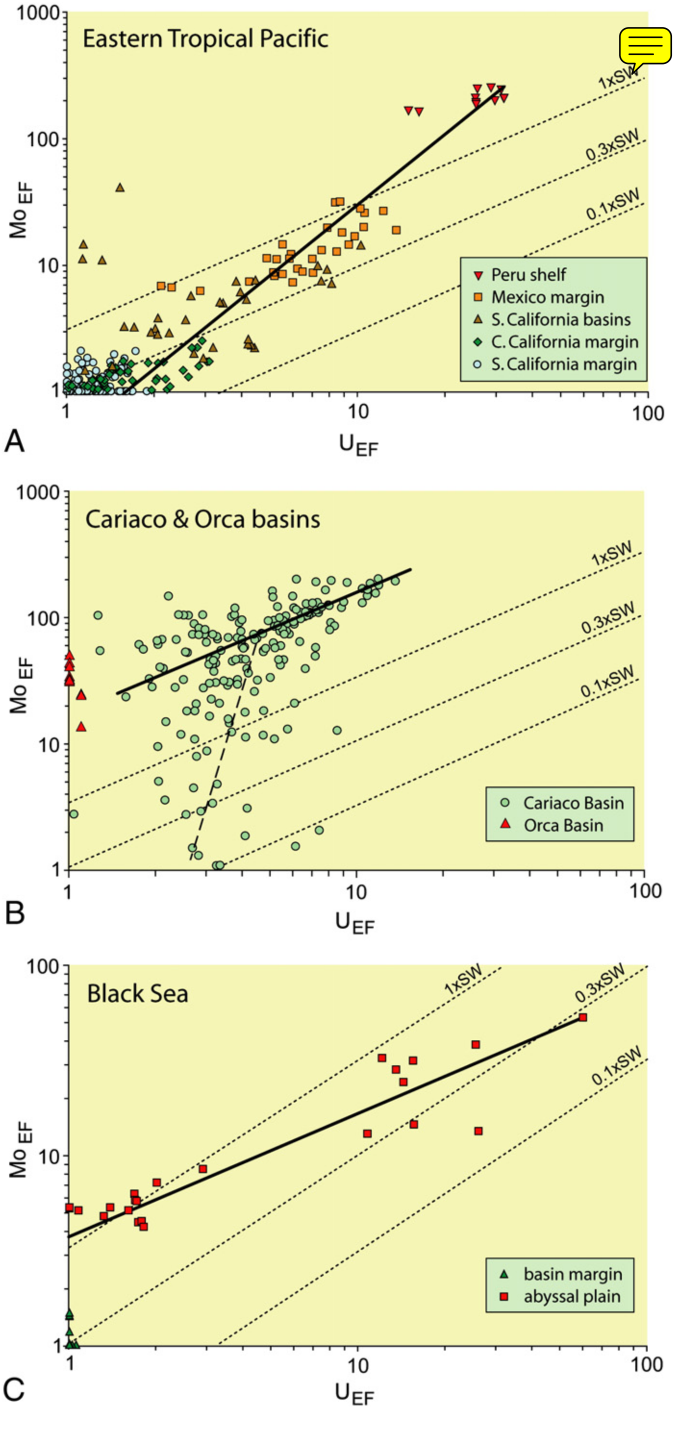

Fig. 4. Mo_{EF} versus U_{EF} for modern marine systems: (A) eastern tropical Pacific, (B) Cariaco and Orca basins, and (C) Black Sea. In C, the basin-margin sites are stations 5, 15, and 17 at water depths of 97–233 m, and the abyssal-plain sites are stations 9, 14, and 18A at water depths of 2094–2218 m. Solid lines show main covariant trends in each dataset, and dashed line in B shows a secondary covariant trend; dotted lines show Mo/U molar ratios equal to the seawater value (1×SW) and to fractions thereof (0.3×SW, 0.1×SW).
Data sources: (A) Irino et al. (2000), Tada et al. (2000), and McManus et al. (2006); (B) Tribovillard et al. (2008) and Riboulleau (unpublished data); (C) Anderson and Fleischer (1991), Barnes and Cochran (1991), and Lyons (1992).

some time before 50 kyr B.P., and the high salinity of the deep watermass is maintained through dissolution of salt in shallow subsurface diapirs in proximity to the basin (Presley and Stearns, 1986; Sheu et al., 1987).

The surface watermass of the Cariaco Basin exhibits aqueous Mo and U concentrations close to those of average seawater (~105 nmol kg^{-1} and ~13.5 nmol kg^{-1}, respectively; Anderson, 1987; Emerson and Huested, 1991). The concentrations of both trace metals decrease downward into the deep watermass, but the decline is larger for Mo (~20%) than for U (~10%; Fig. 3B). Most of the water column exhibits Mo/U molar ratios close to the seawater ratio of ~7.5–7.9, although the deeper part of the water column (~1000–1200 m) shows slightly lower values (6.9 ± 0.6). No aqueous Mo–U concentration data are available for the Orca Basin. The oxic portion of the water column above ~2200 m is unlikely to be modified relative to "normal" seawater, but the chemistry of the highly saline (~360 ppt), dense deep watermass at 2200–2400 m may be evolved.

The Cariaco Basin samples used in this study are from the 528-cm-long Calypso square core (CASQ) MD03-2625, which was recovered from the central saddle of the basin (10° 40.65 N, 64° 58.24 W) at a water depth of 847 m during Leg 1 of the PICASSO expedition (R/V Marion Dufresne). Samples were analyzed for Mo, U, and other trace metals by ICP-MS (Riboulleau, unpublished data). The Orca Basin samples were from a core taken at a depth of 2240 m during the same research expedition, and 10 samples from the upper 7.5 m of the core were analyzed for Mo, U, and other trace metals by ICP-MS (Tribovillard et al., 2008).

2.1.3. Black Sea

The Black Sea, the largest anoxic silled basin in the modern world, has an area of 423,000-km^2 and abyssal plain depths of >2000 m (Degens and Ross, 1974). It is a restricted, hyposaline (18–22‰ salinity) ocean basin with a shallow (~30–35 m) sill connecting it to the Mediterranean Sea via the Bosporus Strait. Water column stratification is maintained by both vertical salinity and temperature gradients. The renewal time (τ_{dw}) of the deep watermass is within the range of ~400 to 2000 yr (Algeo and Lyons, 2006). The O_2/H_2S interface is presently at ~50 m in the basin center and ~120–150 m around the basis margins (Fig. 1C). The chemocline has shallowed since the 1960s, although geologic evidence indicates that its position fluctuated in the pre-modern period as well (Murray et al., 1989; Tugrul et al., 1992; Lyons et al., 1993; Anderson et al., 1994; Wilkin and Arthur, 2001). Below the chemocline, $[H_2S]_{aq}$ increases downward to a maximum of ~400–600 µM in the deep watermass. Organic carbon accumulation rates are generally low (~0.1–1 g cm^{-2} kyr^{-1}) but increase somewhat toward the basin margins (Karl and Knauer, 1991; Calvert et al., 1991; Arthur et al., 1994). Deepwater anoxia is maintained primarily by the strength of water-column stratification and low rates of dissolved oxygen penetration into the deep watermass, and only secondarily by the sinking flux of organic matter.

Aqueous Mo concentrations in the surface watermass are 30–40 nmol kg^{-1}, which is ~0.7 that of average seawater on a salinity-normalized basis (Fig. 3C; Anderson et al., 1989; Emerson and Huested, 1991). Mo concentrations decrease sharply downward below the chemocline, reaching deepwater values of 2–3 nmol kg^{-1}, or only ~0.04 that of seawater on a salinity-normalized basis. Aqueous U concentrations exhibit a modest decrease from surface waters (~8-9 nmol kg^{-1}) into deep waters (~5 nmol kg^{-1}), representing a decline from ~1.0 to ~0.6 times the salinity-normalized seawater value. The far larger decrease in $[Mo]_{aq}$ relative to $[U]_{aq}$ results in a substantial decline in aqueous Mo/U molar ratios, from ~4–5 in the surface watermass to ~0.3–0.5 in the deep watermass. As a fraction of the seawater Mo/U molar ratio, aqueous Mo/U ratios in the Black Sea decrease from ~0.6–0.7 in the surface watermass to ~0.04–0.06 in the deep watermass.

The sediment Mo and U concentration data for the Black Sea (Fig. 4C) were taken from Anderson and Fleischer (1991), Barnes and Cochran (1991), and Lyons (1992). Stations 5, 15, and 17 are basin-margin sites located just above or below the chemocline, at water depths of 233, 198, and 97 m, with average carbonate-free TOC values of 2.8%, 1.9%, and 1.1%, respectively. Stations 9, 14, and 18A are abyssal plain sites at water depths of 2094, 2218, and 2150 m, with average carbonate-free TOC values of 12.8%, 10.2%, and 4.6%, respectively (Lyons, 1992). Sample depths at each station range from the sediment/water interface downward ~20 to 40 cm, representing coccolith oozes and "turbidites" of Unit 1, deposited since ~1320 yr B.P, although the underlying Unit 2 may be present in the Station 18A box core (Lyons, 1992). At any given site, the muddy "turbidite" layers exhibit markedly lower TOC and trace-metal concentrations than the enclosing pelagic sediment, consistent with their derivation from shallower (less reducing) facies.

2.2. Mo–U relationships

The three modern low-oxygen marine systems examined here each show a different and unique pattern of sediment authigenic Mo–U covariation. Sediments from multiple continent-margin sites in the eastern tropical Pacific exhibit a well-defined covariant trend (Fig. 4A, solid line), reflecting variation in Mo_{auth} and U_{auth} concentrations that closely mirrors patterns of redox variation (Fig. 2). Increasingly reducing conditions yield progressively higher Mo_{auth} and U_{auth} concentrations in the following sequence: southern and central California shelves, southern California Borderland basins, Mexican Margin, and Peru Shelf (Fig. 4A; n.b., Mo isotopic variation among these sites shows the same sequence, indicating that $\delta^{98}Mo$ may be a good proxy for temporally integrated redox conditions; Poulson et al., 2006). Samples showing lesser degrees of total authigenic enrichment display modest U_{auth} enrichment but little or no Mo_{auth}, yielding $(Mo/U)_{auth}$ ratios about 0.2–0.5 that of seawater. As total authigenic enrichment increases, samples become progressively more enriched in Mo_{auth} relative to U_{auth}, yielding $(Mo/U)_{auth}$ ratios that range upward to a maximum about 3 times that of seawater (Fig. 4A).

Cariaco Basin sediments are considerably more enriched in Mo_{auth} relative to U_{auth}, and most samples plot well above the seawater Mo/U molar ratio (Fig. 4B). These samples define a trend roughly parallel to the seawater Mo/U trend, representing a $(Mo/U)_{auth}$ ratio about 5 times that of seawater (thick solid line). A subset of samples exhibits a lesser degree of Mo_{auth} enrichment and yields $(Mo/U)_{auth}$ ratios equal to or less than that of seawater. Whether this subset represents a trend (thin dashed line) reflecting changes in $(Mo/U)_{auth}$ ratios as total trace-metal enrichment increased due to an evolution of basinal deepwaters toward more reducing conditions is uncertain. Orca Basin sediments also exhibit strong enrichment of Mo_{auth} (EFs of 10 to 50) relative to U_{auth} (EFs < 2), yielding $(Mo/U)_{auth}$ ratios of ~2 to 8 (Fig. 4B).

Black Sea sediments from basin-margin sites proximal to the chemocline exhibit little or no Mo_{auth} and U_{auth} enrichment (Fig. 4C, triangles), whereas those accumulating at abyssal-plain sites show moderate but variable degrees of enrichment (squares). The latter group exhibits a pronounced covariant trend (solid line) such that samples having lesser degrees of total authigenic enrichment are markedly more enriched in Mo_{auth} than U_{auth}, yielding $(Mo/U)_{auth}$ ratios roughly the same as that of seawater, and samples having greater degrees of total authigenic enrichment yield lower $(Mo/U)_{auth}$ ratios (~0.3–0.6 times the seawater value). This pattern reflects a progressive enrichment of U_{auth} relative to Mo_{auth} as total authigenic concentrations increase.

2.3. Interpretations

Differences in the authigenic Mo–U covariation patterns of modern low-oxygen marine systems (Fig. 4) suggest that multiple factors may be influencing uptake of authigenic trace metals by the sediment. Likely controls fall into three categories: (1) benthic redox conditions, including both the mean redox state and the degree of redox variability, (2) operation of particulate shuttles that could accelerate removal of trace metals to the sediment, and (3) changes in the chemistry of the overlying water column, especially its aqueous Mo/U ratio (Fig. 5). Although conceptually separate, these three controls are in fact commonly interdependent in nature.

Benthic redox conditions are generally recognized as a dominant influence on the accumulation of authigenic trace metals in the sediment. The tropical eastern Pacific system examined in this study

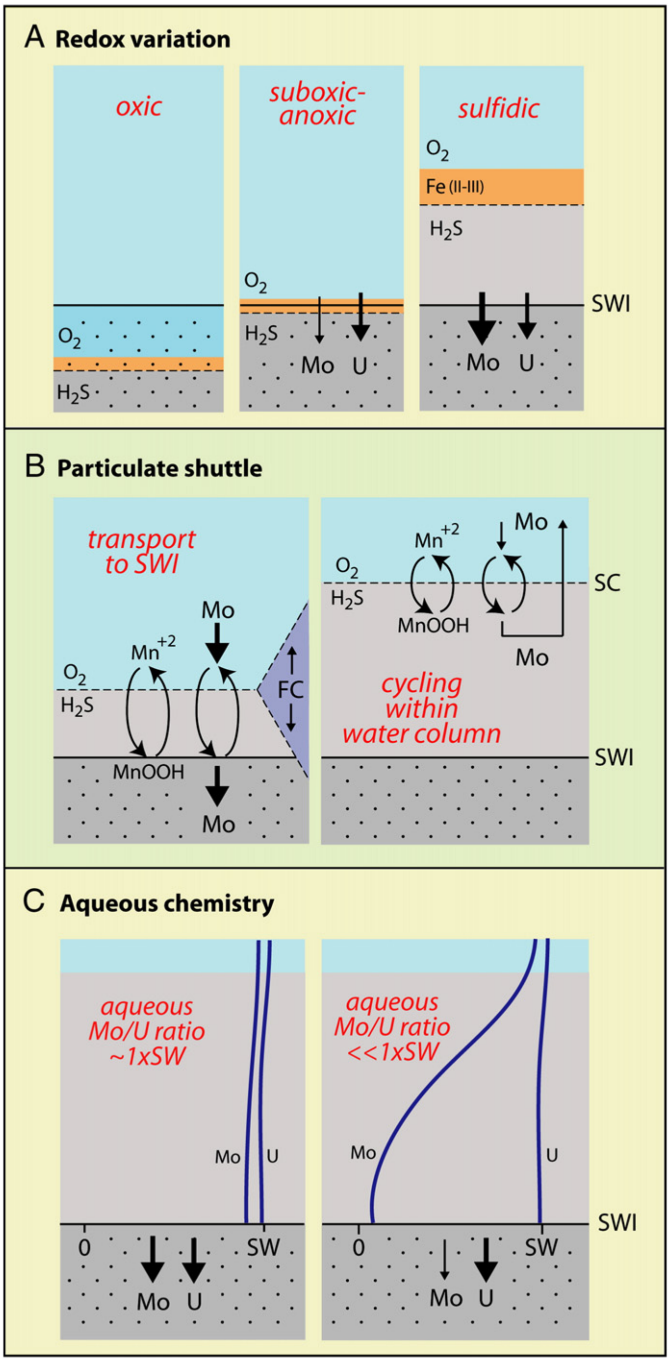

Fig. 5. Cartoon showing relationships of Mo and U authigenic enrichment to (A) benthic redox variation, (B) Mn-oxyhydroxide particulate shuttle, and (C) evolving aqueous chemistry. In A, the zone of aerobic respiration is shown in blue, the (generally narrow) field of anoxic–nonsulfidic conditions (zones of Fe(III), Mn(IV) and nitrate reduction in orange, and the zone of sulfate reduction in gray. In B, MnOOH and Mn^{+2} represent the downward flux of particulate Mn-oxyhydroxides and the upward flux of aqueous reduced Mn, respectively; Mo represents the flux of adsorbed molybdate to the sediment (left panel) and its recycling within the water column (right panel); FC and SC represent fluctuating and stable chemocline depths, respectively. In C, the x-axis scale relates to aqueous Mo and U vertical concentration profiles and ranges from zero to the seawater (SW) value. In A–C, size of arrows shows relative magnitudes of authigenic Mo and U fluxes to the sediment. SWI = sediment/water interface. See text for discussion.

comprises unrestricted (or weakly restricted) marine sites in which benthic redox conditions range from well oxygenated to strongly oxygen depleted (i.e., anoxic and intermittently sulfidic). The relationship of redox conditions to authigenic Mo–U enrichment in this system is fairly unambiguous: (1) oxic facies exhibit little or no enrichment, (2) suboxic facies exhibit modest enrichment with $(Mo/U)_{auth}$ ratios distinctly lower than the seawater ratio, and (3) anoxic facies exhibit strong enrichment accompanied by progressively higher $(Mo/U)_{auth}$ ratios as total authigenic concentrations increase (Fig. 4A). This pattern is consistent with well-understood controls on trace-metal uptake by sediments. Under suboxic conditions, U_{auth} is taken up preferentially over Mo_{auth} because U(VI) is reduced at the Fe(II)–Fe(III) redox boundary, prior to the onset of sulfate reduction, which controls Mo_{auth} accumulation (Fig. 5A; Morford and Emerson, 1999; Zheng et al., 2002a; Morford et al., 2005). Although the redox zone in which Fe is reduced is typically narrow within the sediment, in marine systems in which the chemocline hovers close to the sediment/water interface substantial uptake of U_{auth} through shallow diffusion may be possible without significant uptake of Mo_{auth}, which must diffuse into the deeper, sulfidic part of the sediment column. Under anoxic conditions, in which the chemocline rises close to (or above) the sediment/water interface, formation of thiomolybdates most likely converts aqueous Mo to a particle-reactive form and enhances the uptake of authigenic Mo by the sediment (Fig. 5A; Helz et al., 1996; Zheng et al., 2000). Such conditions result in rates of uptake of Mo_{auth} that substantially exceed those of U_{auth}, resulting in a progressive increase in sediment $(Mo/U)_{auth}$ ratios as EFs increase (e.g., Fig. 4A). Transient (<5 yr) episodes of enhanced anoxia in mildly restricted basins, such as in the Santa Barbara Basin where such changes have been linked to ENSO forcing of ventilation, can result in substantial short-term increases in the flux of Mo_{auth} to the sediment (Zheng et al., 2000).

Additional controls on authigenic Mo–U accumulation must be invoked to explain features of the datasets from the Cariaco and Orca basins and the Black Sea. The strong relative enrichment of Mo_{auth} relative to U_{auth} in the Cariaco and Orca basins (Fig. 4B) is probably due to operation of a "particulate shuttle" linked to Mn–Fe redox cycling within the water column, a process known to operate in both the Cariaco Basin (de Baar et al., 1988; Ho et al., 2004) and the Orca Basin (Trefry et al., 1984; Van Cappellen et al., 1998). The effectiveness of a particulate shuttle in promoting Mo_{auth} accumulation may be enhanced by strong variation in water-column redox conditions at short to intermediate timescales. The deepwater residence time of the Cariaco Basin is ~50–100 years (Algeo and Lyons, 2006), and observational data show that major renewal events occur at intervals of years to decades (Zhang and Millero, 1993; Scranton et al., 2001; Ho et al., 2004). In the Orca Basin, a particulate shuttle may be the main vector for trace-metal enrichment of the sediment. In contrast to Mo, most redox-sensitive trace metals, including U, Cu, Ni, Zn, Pb, and Cd, show little or no enrichment, suggesting limited uptake across the sediment/water interface possibly owing to low concentrations of these metals in the deep watermass (the "basin reservoir effect"; Tribovillard et al., 2008). Mo is enriched in Orca Basin sediments despite possible drawdown in the deep watermass because it is continuously scavenged by Mn-oxyhydroxides within the redox transition zone (2200–2250 m; Trefry et al., 1984; Van Cappellen et al., 1998). The importance of particulate shuttles in enhancing Mo_{auth} uptake in largely unrestricted continent-margin settings with intermittently sulfidic bottomwaters (such as the eastern tropical Pacific) is less clear. However, a fraction of the Mo_{auth} flux (≤15%) to the sediment in the Santa Barbara Basin has been attributed to such a particulate shuttle (Zheng et al., 2000).

An additional factor may influence authigenic Mo–U enrichment patterns in the Black Sea: evolution of the watermass chemistry. Unlike both the eastern tropical Pacific and the Cariaco Basin, in which aqueous Mo/U molar ratios are generally close to that of seawater (~7.5–7.9), aqueous Mo/U ratios in the Black Sea decrease from 4.6–4.9 in the surface watermass rapidly downward below the chemocline to a minimum of ~0.3 (Fig. 3C). Thus, substantially less dissolved Mo is available for uptake by sediments in slope and basinal areas of the Black Sea than at sites bathed in seawater of "normal" chemistry. That the signal of the evolved chemistry of Black Sea deepwaters can be recorded by sediment Mo/TOC ratios was demonstrated by Algeo and Lyons (2006). This signal may also be apparent in a Mo_{EF}–U_{EF} crossplot, which shows a distinct trend toward lower $(Mo/U)_{auth}$ ratios with increasing total authigenic enrichment (Fig. 4C). The relationship of this trend to the seawater molar ratio line (1×SW) is unambiguously different from that for open-marine systems (Fig. 4A) and at odds with expectations of enhanced Mo_{auth} accumulation in sulfidic restricted basins (e.g., Fig. 4B). The most likely explanation for this pattern is that sites exhibiting lower $(Mo/U)_{auth}$ ratios accumulated under the influence of the Mo-depleted deep watermass (Mo/U molar ratio ~0.3–0.5), and sites yielding higher $(Mo/U)_{auth}$ ratios were exposed to the (relatively) Mo-enriched surface watermass (Mo/U molar ratio ~2–5; Fig. 3C).

The foregoing discussion allows some generalizations concerning patterns of authigenic Mo–U enrichment in different types of low-oxygen marine systems (Fig. 6). In unrestricted marine systems such as continent-margin upwelling systems, a shift from suboxic to sulfidic benthic redox conditions enhances uptake of both Mo_{auth} and U_{auth}, but relatively stronger accumulation of Mo_{auth} results in a progressive increase in $(Mo/U)_{auth}$ ratios from 0.1–0.3 times the seawater molar ratio to 1.0–3.0 times that ratio. This pattern reflects the preferential uptake of U_{auth} over Mo_{auth} when redox conditions at the sediment/water interface hover around suboxic, and of Mo_{auth} over U_{auth} when benthic redox conditions are strongly and/or frequently sulfidic. In euxinic silled basins, patterns of authigenic Mo–U enrichment depend on whether a particulate shuttle is operative, which in turn depends on the size of the basin and the height and stability of its chemocline. In smaller basins characterized by a deep or highly variable chemocline, operation of a particulate shuttle is likely to enhance transfer of aqueous Mo to the sediment/water interface, resulting in elevated and relatively uniform $(Mo/U)_{auth}$ ratios. In larger basins characterized by a shallow and stable chemocline, a particulate shuttle is unlikely to be effective at delivering Mo to the sediment/water interface. In these systems, relative rates of authigenic Mo–U enrichment will depend on the degree of evolution of its water chemistry (a natural consequence of the highly restricted character of the basin and the long residence time of its deep watermass). Initially, when the aqueous Mo/U molar ratio is close to that of seawater, sediment $(Mo/U)_{auth}$ ratios will be

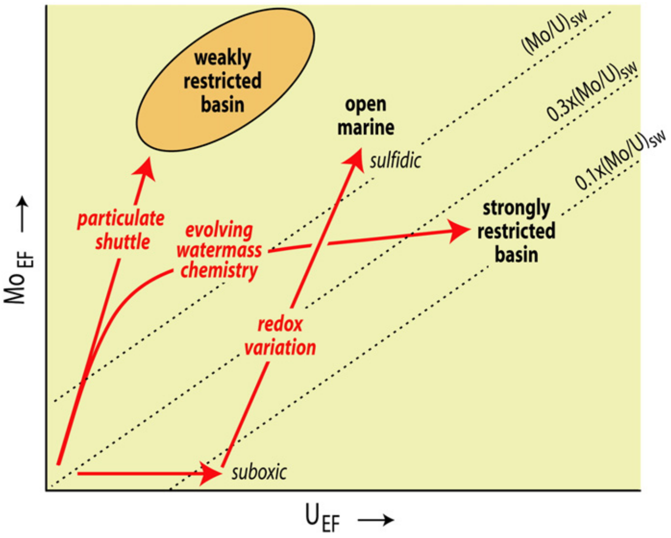

Fig. 6. Model of enrichment patterns and changes in $(Mo/U)_{auth}$ ratios in response to the controls illustrated in Fig. 4. The diagonal dotted lines represent the seawater (SW) Mo/U molar ratio of ~7.5–7.9 and fractions thereof. See text for discussion.

high, but as aqueous Mo is depleted through sedimentation without compensatory resupply, sediment $(Mo/U)_{auth}$ ratios will decline proportionately.

3. Mo–U covariation in ancient marine systems

Authigenic Mo–U relationships in modern low-oxygen marine systems have the potential to serve as a basis for analysis of environmental conditions and processes in ancient low-oxygen marine systems. In the following, we examine two case studies, the Late Pennsylvanian Midcontinent Sea and the Late Devonian Seaway of the North American craton.

3.1. Late Pennsylvanian Midcontinent Sea (LPMS)

The LPMS was a large, nearly landlocked cratonic-interior sea bordered by the lowlying Laurentian craton to the north and east, the Appalachian and Ouachita orogens to the south, and the Ancestral Rocky Mountains to the west (Fig. 7; Heckel, 1977; Algeo and Heckel, 2008; Algeo et al., 2008). It was located at 0 to 15°N paleolatitude within the paleo-intertropical convergence zone, producing a monsoonal climate with moisture-laden air masses drawn from the proto-Tethyan embayment to the east (Crowley et al., 1989; Parrish, 1993; Poulsen et al., 2007; Montañez et al., 2007). Strong precipitation and runoff, especially in the Appalachian Basin region, produced a

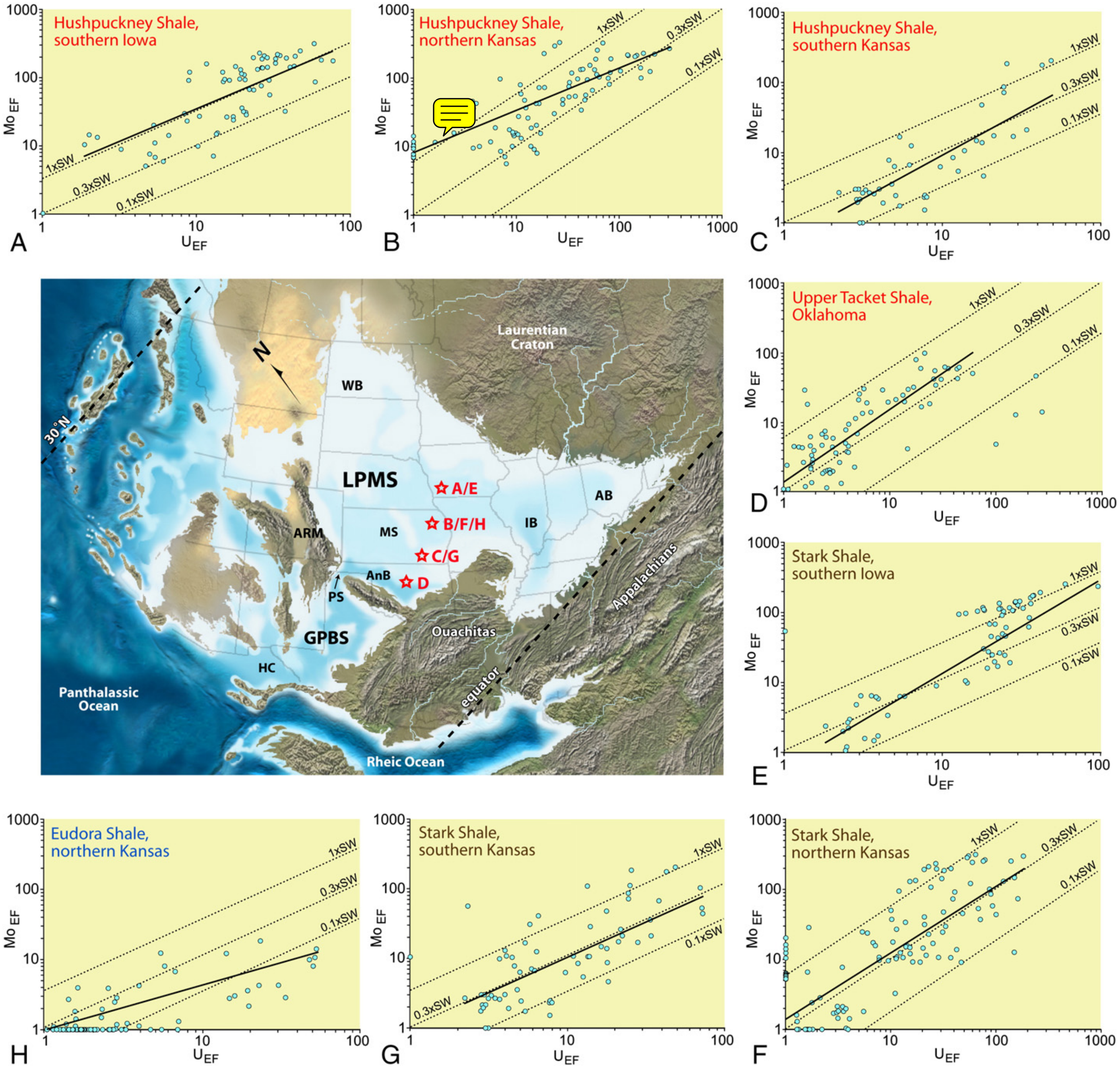

Fig. 7. Mo_{EF} versus U_{EF} for Late Pennsylvanian Midcontinent Sea. (A–C) Hushpuckney Shale, (D) Upper Tacket Shale (lateral equivalent of Hushpuckney), (E–G) Stark Shale, and (H) Eudora Shale. Solid lines show main covariant trends in each dataset; dotted lines show Mo/U molar ratios equal to the seawater value (1×SW) and to fractions thereof (0.3×SW, 0.1×SW). Data sources: Algeo and Maynard (2004) and Algeo (unpublished). Paleogeographic map modified from Algeo et al. (2008). Geographic abbreviations: AB = Appalachian Basin, AnB = Anadarko Basin, ARM = Ancestral Rocky Mountains, GPBS = Greater Permian Basin Seaway, HC = Hovey Channel, IB = Illinois Basin, LPMS = Late Pennsylvanian Midcontinent Sea, MS = Midcontinent Shelf, PS = Panhandle Strait, WB = Williston Basin.

reduced-salinity surfacewater layer extending from the eastern interior of the LPMS westward to at least the Midcontinent Shelf and contributed to the development of a large-scale "superestuarine" circulation pattern, characterized by a strong water-column pycnocline and pronounced spatial gradients in environmental and sedimentary parameters (Hoffman et al., 1998; Algeo and Heckel, 2008; Algeo et al., 2008). The laterally unconfined character of the pycnocline resulted in high-frequency fluctuations in watermass properties at relatively short (i.e., decadal to millennial) timescales, especially with regard to redox conditions, nutrient upwelling rates, and primary productivity (Algeo et al., 2008; Algeo and Heckel, 2008). Benthic redox conditions in the Midcontinent Shelf region fluctuated between suboxic and strongly sulfidic (Algeo et al., 2004; Algeo and Maynard, 2004).

Bathymetric variation within the Midcontinent region was relatively limited, although local areas of positive relief existed around the Central Kansas and Nemaha uplifts and the Bourbon and Mississippi River arches. The Trancontinental and Siouxian arches were shallowly submerged structural highs that separated the Midcontinent Shelf from the Williston Shelf to the north (Fig. 7). The average depth of the entire LPMS was estimated at ~50 m, although southern portions of the Midcontinent Shelf may have been as deep as ~150 m (Algeo and Heckel, 2008). Water depths in the adjacent Arkoma and Anadarko foredeep basins to the southwest were generally greater (hundreds of meters) but varied through time in response to episodes of basin subsidence and fill (Arbenz, 1989). The principal connection of the LPMS to the global ocean was at the northwest end of the Anadarko–Dalhart basins, where the Panhandle Strait led to the Palo Duro and Midland basins and thence to the Hovey Channel and eastern tropical Panthalassic Ocean (Fig. 7; Algeo et al., 2008). This connection is thought to have been a continuous, ~1000-km-long deepwater corridor deepwater, although water depths over structural sills separating these basins are poorly known.

Patterns of authigenic Mo–U covariation were examined for three Upper Pennsylvanian black shales from the Midcontinent region: (1) the Hushpuckney Shale (Swope Formation) and its lateral equivalent, the Upper Tacket Shale, (2) the Stark Shale (Dennis Formation), and (3) the Eudora Shale (Stanton Formation). The Hushpuckney and Stark shales belong to the lower part of the Missourian Stage (first half of the Late Pennsylvanian), and the Eudora Shale to the upper part of the same stage (Heckel, 1977). All three horizons represent "core" shales of Midcontinent cyclothems, deposited during three separate interglacial highstands of the LPMS. The highstands of the early Missourian Stage (Hushpuckney and Stark) were characterized by greater water depths, stronger pycnoclines, and more reducing benthic redox conditions on the Midcontinent Shelf than those of the late Missourian Stage (Eudora), as indicated by the geographic extent of black shale deposition and redox proxies such as DOP, TOC, and trace-metal concentrations.

The three study horizons exhibit some common features with regard to authigenic Mo–U accumulation: (1) variable but commonly high EFs, (2) $(Mo/U)_{auth}$ ratios that are mostly between 0.1 and 1 times that of seawater, and (3) little variation in $(Mo/U)_{auth}$ ratios with increasing EFs at a given site (yielding covariation trend lines nearly parallel to the seawater molar ratio lines; Fig. 7A–H). For the Hushpuckney and Upper Tacket shales, regular spatial variation is apparent among the study sites: (1) average EFs decline in moving from northeast to southwest across the LPMS, and (2) average $(Mo/U)_{auth}$ ratios decline from ~1×SW at the northernmost site (southern Iowa) to ~0.3–0.4×SW at the southernmost sites (southern Kansas and Oklahoma). For the Stark Shale, little spatial variation is evident: the ranges of EFs for Mo_{auth} and U_{auth} are similar, and all three sites yield average $(Mo/U)_{auth}$ ratios of ~0.3×SW with no apparent relationship to variation in EFs (Fig. 7E–G). The Eudora Shale exhibits substantially lower EFs than the other units: <20 for Mo_{auth} and <50 for U_{auth} (Fig. 7H). Further, $(Mo/U)_{auth}$ ratios decrease from ~0.3×SW to ~0.1×SW as EFs increase, yielding some of the lowest $(Mo/U)_{auth}$ ratios among any of the LPMS study units.

The authigenic Mo–U enrichment patterns for the LPMS study units do not closely match those for any of the modern marine systems considered above, although patterns of spatial variation in the Hushpuckney–Tacket (Fig. 7A–D) may provide some insights regarding controls on Mo–U accumulation. Increasing $(Mo/U)_{auth}$ ratios and higher EFs to the northeast suggest that redox conditions were more reducing to the interior regions of the LPMS (cf. Hoffman et al., 1998; Algeo and Heckel, 2008). However, the individual LPMS study sites do not yield sets of tightly clustered samples, nor do they collectively show a progression from low $(Mo/U)_{auth}$ ratios at lower EFs to high $(Mo/U)_{auth}$ ratios at higher EFs (Fig. 7A–H), both of which are features of the modern tropical eastern Pacific (Fig. 4A). The pattern of authigenic Mo–U covariation in the LPMS is suggestive of highly variable redox conditions, probably ranging over the full redox spectrum (from oxic or suboxic to sulfidic) at each of the study sites, an inference consistent with the results of earlier studies (Hoffman et al., 1998; Algeo et al., 2004; Algeo and Maynard, 2004; Algeo and Heckel, 2008). Such strong variability in redox conditions across a wide region of the LPMS is consistent with the inference of a shallow and laterally unbounded pycnocline, the strength and spatial extent of which varied through time in response to changes in region humidity and freshwater discharge into this nearly landlocked cratonic sea (Algeo et al., 2008, their figure 9). High-frequency changes in redox conditions within the LPMS (Algeo et al., 2004) may have resulted in early post-depositional remobilization of Mo and U, a process likely to attenuate primary depositional relationships and yield broadly irregular covariant trends of the type seen in many of the LPMS study units (Fig. 7).

Most LPMS samples yield $(Mo/U)_{auth}$ ratios less than that of modern seawater (although a few yield ratios as high as ~3×SW; Fig. 7A–H), in contrast to modern open-ocean and silled-basin marine systems in which strongly reducing conditions result in most samples having $(Mo/U)_{auth}$ ratios substantially higher than the seawater molar ratio (Fig. 4A–B). There are several possible explanations for this observation. First, deepwaters welling up on the southwestern margin of the LPMS may have been depleted in Mo as a consequence of their transit through a ~1000-km-long, anoxic deepwater corridor in the Greater Permian Basin region, during which Mo may have been removed to the sediment (Algeo et al., 2008; Algeo and Heckel, 2008). This mechanism is analogous to the aqueous Mo depletion process operating in the modern Black Sea, although the oceanographic details differ, and seems to be the most likely explanation. A second possibility is that global seawater had a lower Mo/U molar ratio during the Carboniferous than at present, although independent evidence to support this hypothesis is lacking. Finally, Mo may have been preferentially remobilized relative to U during the frequent oxygenation events that affected the Midcontinent Shelf, leading to reduced sediment $(Mo/U)_{auth}$ ratios. Although both Mo_{auth} and U_{auth} are subject to some degree of remobilization along oxidation fronts that penetrate into anoxic sediments (Thomson et al., 1995, 1998; Chaillou et al., 2002, 2008), there is at present no empirical data to suggest that Mo_{auth} would be lost at higher rates than U_{auth}.

3.2. Late Devonian Seaway (LDS)

The LDS extended across the North American craton from the Acadian Orogen at ~30°S paleolatitude to the Cordilleran Geosyncline close to the paleoequator (Fig. 8). Climate conditions were relatively dry owing to the orogenic rainshadow effect of the Acadian Mountains to the south and east (Ettensohn and Barron, 1983; Woodrow, 1985; Ettensohn, 1985). The craton was subdivided by structural highs into a series of basins, including the Appalachian and Black Warrior basins south of the Cincinnati Arch, the Michigan, Illinois, Iowa, and Oklahoma basins north of the Cincinnati Arch and south of the Transcontinental Arch, and the Williston and Elk Point basins north of

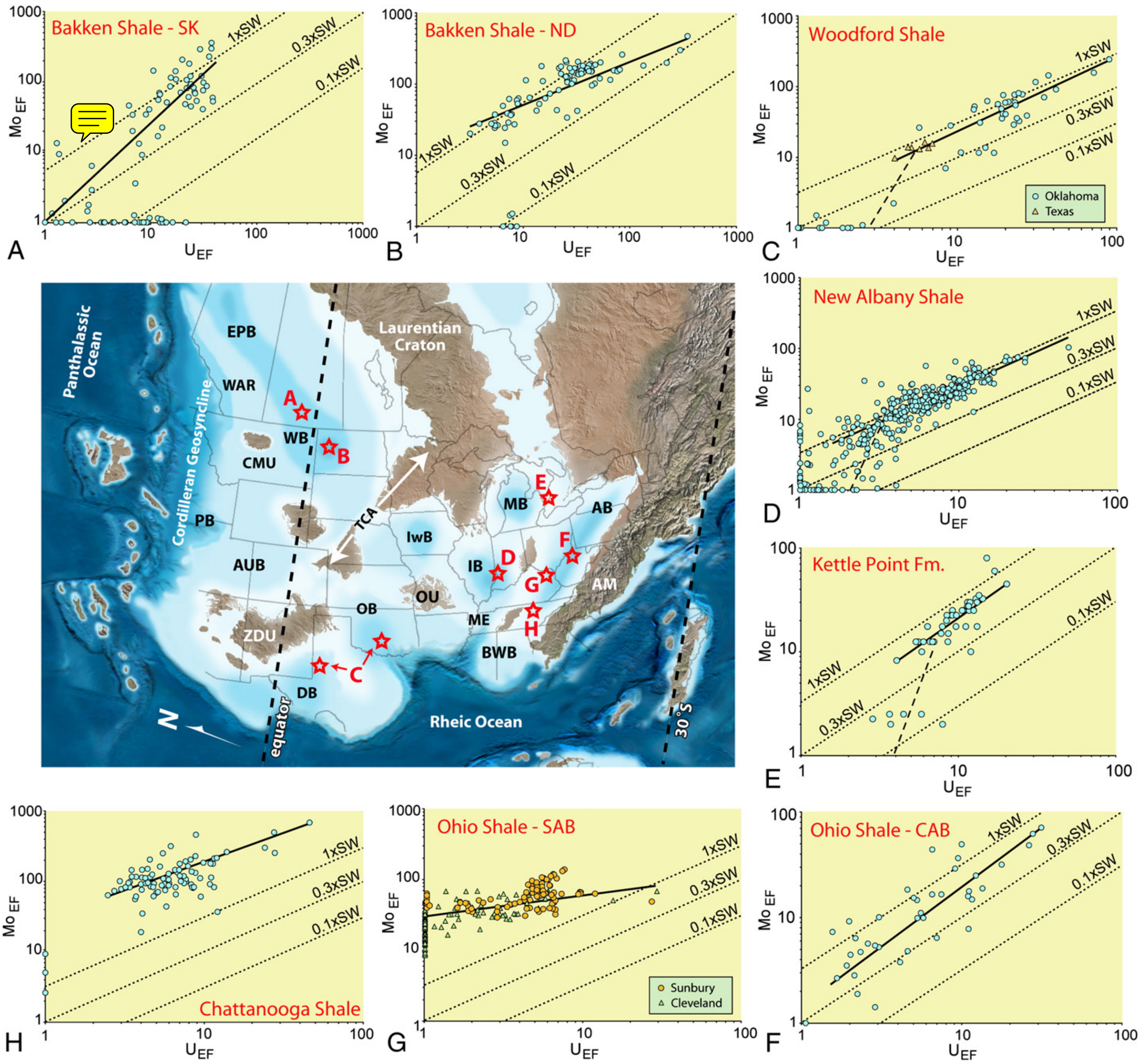

Fig. 8. Mo$_{EF}$ versus U$_{EF}$ for Late Devonian Seaway: (A) Bakken Shale-SK (Saskatchewan), (B) Bakken Shale-ND (North Dakota), (C) Woodford Formation, (D) New Albany Shale, (E) Kettle Point Formation, (F) Ohio Shale-CAB (Central Appalachian Basin), (G) Ohio Shale-SAB (Southern Appalachian Basin), and (H) Chattanooga Shale. Solid lines show main covariant trends in each dataset, and dashed lines show secondary covariant trends; dotted lines show Mo/U molar ratios equal to the seawater value (1×SW) and to fractions thereof (0.3×SW, 0.1×SW).

Data sources: (A) Karma (1991), (B) Hartwell (1998); (C) Algeo and Over (unpublished); (D) Frost et al. (1985); (E) Armstrong (1986); (F) Leventhal and Hosterman (1982); (G) Jaminski (1997); and (H) Rheams and Neathery (1988). Paleogeographic map modified from Algeo et al. (2007). Geographic abbreviations: AB = Appalachian Basin, AM = Appalachian Mountains, AUB = Ancestral Uinta Basin, BWB = Black Warrior Basin, CA = Cincinnati Arch, CMU = Central Montana Uplift, DB = Delaware Basin, EPB = Elk Point Basin, IB = Illinois Basin, IwB = Iowa Basin, MB = Michigan Basin, ME = Mississippi Embayment, OB = Oklahoma Basin, OU = Ozark Uplift, PB = Pilot Basin, TCA = Trans-Continental Arch, WAR = West Alberta Ridge, WB = Williston Basin, ZDU = Zuni-Defiance Uplift.

the Transcontinental Arch (Fig. 8). The existence of these structural features during the Late Devonian was due to reactivation of basement faults associated with compressional stress fields set up by the Acadian Orogeny (Howell and van der Pluijm, 1990, 1999; cf. Zoback and Zoback, 1991), possibly reflecting the slide of the craton into a geoid low during the formation of the Pangean supercontinent (Bond and Kominz, 1991).

As a consequence of these structural features, substantial bathymetric variation existed across the LDS. Although absolute water depths cannot be determined, the deeper parts of the Appalachian Basin accumulated laminated hemipelagic sediments, probably at water depths up to a few hundred meters (Potter et al., 1982; Jaminski et al., 1998; Werne et al., 2002; Sageman et al., 2003). The other cratonic-interior basins were not as deep but still probably below wave base (>~50 m). In contrast, the shallow sills between these basins accumulated successions characterized by current and wave structures, lag deposits, erosion surfaces, and oolitic ironstones, indicative of shallow water depths (<50 m, and perhaps <20 m) (Schieber, 1994a,b,c, 1998a,b; Schieber and Riciputi, 2004). Water depths across the LDS varied by meters to a few tens of meters in response to secular eustatic fluctuations at timescales of ~10^4–10^6 yr (Johnson et al., 1985; Haq and Schutter, 2008). Such sea-level fluctuations appear to have left a distinctive sedimentological signature in areas of shallow sills (Schieber, 1998a; Schieber and Riciputi, 2004).

Owing to its pronounced bathymetric variation, the LDS represents a rather different type of paleoceanographic system than the LPMS. Although no detailed analysis of its hydrographic dynamics has been undertaken to date, some inferences follow logically from the conditions outlined above. Although surface waters were probably in communication across the LDS, deep waters in many basins were restricted to varying degrees, resulting in long deepwater residence times and the chemical evolution of deep watermasses. Deepwater residence times, estimated on the basis of Mo/TOC ratios, ranged from decades to hundreds of years in different basins and varied somewhat through time within individual basins in response to eustatic and tectonic forcings (Algeo et al., 2007). The chemical evolution of the watermass of some basins in response to deepwater restriction may be evidenced by changing ratios among redox-sensitive trace metals (Algeo and Maynard, 2008). The development of local chemical signatures in (semi-)restricted watermasses (termed "aquafacies") has been documented in other cratonic systems as well (Holmden et al., 1998; Panchuk et al., 2005; Immenhauser et al., 2008). A recent attempt at a comprehensive paleoceanographic analysis of the LDS (Perkins et al., 2008) completely disregarded the potential influence of bathymetric variation on watermass restriction and, hence, is of limited value.

Upper Devonian black shales from the LDS exhibit a variety of authigenic Mo–U covariation patterns (Fig. 8). The only commonality among these diverse patterns is that all show positive covariation between Mo_{auth} and U_{auth} concentrations. More revealing are the differences among the various study units, which can potentially provide insights regarding environmental conditions and processes within the individual basins of the LDS.

Black shales of the Bakken/Exshaw Formation are generally strongly enriched in Mo_{auth} and U_{auth}, with $(Mo/U)_{auth}$ ratios mostly between 0.5 and 2 times the seawater molar ratio (Fig. 8A–B). Studies of this formation in the northern and southern Williston Basin yield slightly different patterns: in Saskatchewan (north) higher EFs are correlated with increasing $(Mo/U)_{auth}$ ratios (Fig. 8A), whereas in North Dakota (south) higher EFs correspond to decreasing $(Mo/U)_{auth}$ ratios (Fig. 8B). Although the significance of these differences is speculative, the observed patterns may reflect spatial variation in hydrographic conditions within the Williston Basin. The authigenic Mo–U covariation pattern for the southern area is similar to that for the modern Black Sea (Fig. 4C), suggesting uniformly sulfidic conditions (owing to strong water-column stratification) coupled with drawdown of aqueous Mo concentrations in the deep watermass. The Mo–U covariation pattern for the northern area resembles more closely that for the modern eastern tropical Pacific (Fig. 4A), suggesting greater benthic redox variation, i.e., ranging from suboxic to sulfidic. These patterns suggest that the southern Williston Basin was deeper than all of the surrounding shelf areas, and that it therefore developed a restricted, permanently sulfidic deep watermass, whereas the northern Williston Basin, which was connected to the open ocean through the Elk Point trough, was shallower and experienced better watermass exchange, resulting in greater benthic redox variability. Thus, spatial variation in authigenic Mo–U patterns of the Bakken/Exshaw Shale may be understood in terms of paleogeographic controls (Fig. 8).

The Woodford Formation, which accumulated on the southern margin of the North American craton, exhibits marked enrichment in both Mo_{auth} and U_{auth} and nearly constant $(Mo/U)_{auth}$ ratios of ~1×SW (Fig. 8C). A subset of samples characterized by lower overall Mo_{auth} and U_{auth} enrichment (EFs$<$3) exhibits lower $(Mo/U)_{auth}$ ratios (0.1–0.3). No difference in authigenic Mo–U patterns is apparent for Woodford samples from the Oklahoma Basin of southern Oklahoma versus the Delaware Basin of western Texas (Fig. 8C). Similar patterns of authigenic Mo–U covariation are shown by the New Albany Shale of the Illinois Basin (Fig. 8D), the Kettle Point Formation of the Algonquin Arch in southern Ontario (Fig. 8E), and the Ohio Shale of the Central Appalachian Basin (Fig. 8F). These formations exhibit only minor differences: (1) lower maximum EFs in the latter units relative to the Woodford Formation, and (2) slightly lower average $(Mo/U)_{auth}$ ratios (~0.5–0.7×SW) in the Kettle Point and Ohio shales relative to the Woodford and New Albany shales. All four formations are inferred to have formed under generally similar conditions, although given the lack of an exact modern analog (cf. Fig. 4), the nature of those conditions is uncertain. The $(Mo/U)_{auth}$ ratios are not sufficiently high to be attributed to the operation of a particulate shuttle (cf. Fig. 4B), and the lack of a trend toward higher $(Mo/U)_{auth}$ ratios with increasing EFs is not consistent with control by variation in redox conditions alone (cf. Fig. 4A). One potential explanation is that the tendency toward higher $(Mo/U)_{auth}$ ratios under more reducing conditions has been offset by lower aqueous Mo concentrations (i.e., similar to the inferred controls on Mo_{auth}–U_{auth} covariation in the Pennsylvanian cyclothemic shales discussed above). This situation might have existed if the interior basins of the North American craton were moderately restricted (i.e., less so than the modern Black Sea), as inferred by Algeo et al. (2007), yet still lacked an effective particulate shuttle. The subsets of samples in the Woodford, New Albany, and Kettle Point formations characterized by low EFs and $(Mo/U)_{auth}$ ratios $<$0.3 (Fig. 8C–E, dashed lines) may reflect preferential uptake of U over Mo under largely suboxic conditions, as observed for the eastern tropical Pacific (Fig. 4A).

In contrast to the units discussed above, the Ohio Shale of the Southern Appalachian Basin and the Chattanooga Shale exhibit a markedly different pattern of authigenic Mo–U covariation (Fig. 8G–H). Both units are strongly enriched in Mo_{auth} relative to U_{auth}, yielding $(Mo/U)_{auth}$ ratios from 3 to 10 times the seawater molar ratio. Strong relative enrichment of Mo_{auth} is indicative of the operation of a particulate shuttle enhancing the transfer of Mo to the seafloor, as in the modern Cariaco Basin (Fig. 4B). The operation of such a shuttle in the Southern Appalachian Basin and across the sill connecting it to the Rheic Ocean to the south implies that the water column in this region experienced frequent redox fluctuations between suboxic and moderately sulfidic conditions (cf. Rimmer, 2004). This inference is consistent with strong but temporally variable watermass exchange across the southern sill of the Appalachian Basin (Algeo et al., 2007). One difference between the authigenic Mo–U covariation patterns for the southern Ohio Shale and the Chattanooga Shale is that the latter yields a covariation trend reflecting a nearly constant $(Mo/U)_{auth}$ ratio (~5×SW), whereas the former exhibits a progressive decline in $(Mo/U)_{auth}$ ratios (from ~5×SW to ~1×SW) as total authigenic enrichment increases (Fig. 8G–H). Although its significance is not certain, this relationship may reflect greater restriction (and, hence, lower aqueous Mo concentrations) of the deep watermass within the Appalachian Basin eastward into the deeper parts of the basin. In contrast, sill areas in central Tennessee may have been sufficiently shallow that little if any vertical change in aqueous chemistry existed within the water column.

4. Conclusions

Patterns of authigenic Mo–U covariation can be related to specific environmental conditions and processes within marine systems, especially with regard to (1) redox variation, (2) operation of particulate Mn–Fe-oxyhydroxide shuttles, and (3) evolution of aqueous trace-metal chemistry in restricted basins. In modern open-ocean systems characterized by suboxic bottomwater conditions, enrichment of U_{auth} tends to exceed that of Mo_{auth} owing to the threshold concentration of H_2S required for conversion of molybdate to particle-reactive thiomolybdate. In open-ocean systems with more strongly reducing bottomwater conditions, both Mo_{auth} and U_{auth} are strongly enriched and $(Mo/U)_{auth}$ ratios increase to or above the Mo/U ratio of seawater (~7.5–7.9). In restricted marine systems with permanently sulfidic deepwaters, the relative enrichment of authigenic Mo and U depends on additional factors. In the Cariaco Basin, the operation of a particulate Mn–Fe-oxyhydroxide shuttle serves to accelerate the transfer of Mo to the seafloor, leading to strong enrichment of Mo_{auth} over U_{auth}. In contrast to the Cariaco Basin, which has an aqueous Mo/U ratio similar to that of seawater, the deepwater Mo/U ratio of the Black Sea is only ~0.04 that of seawater owing to elevated rates of Mo removal to the sediment without compensatory resupply. As a consequence, abyssal-plain sediments in the Black Sea exhibit lesser degrees of enrichment of Mo_{auth} relative to U_{auth} and $(Mo/U)_{auth}$ ratios smaller than the seawater ratio of ~7.5–7.9. Inferences concerning redox and hydrographic controls on authigenic Mo–U accumulation in modern low-oxygen marine systems can be applied to an analysis of environmental conditions and processes in ancient low-oxygen marine systems. Analysis of authigenic Mo–U covariation in Paleozoic black shales from the North American craton allows delineation of spatial variation in the roles of redox intensity, particulate shuttles, and watermass chemical evolution within the Late Pennsylvanian Midcontinent Sea and the Late Devonian Seaway. The observed patterns are consistent with laterally unconfined circulation and strong watermass exchange within the LPMS, and with markedly restricted deepwater circulation in silled basins of the LDS.

Acknowledgments

Thanks to Armelle Riboulleau for the unpublished Mo–U data from the Cariaco Basin, to Jeffrey Over for samples of the Woodford Formation, to Tim Lyons for comments on an early draft of the manuscript, and to the Iowa, Kansas, Oklahoma, North Dakota, Kentucky, and Ohio state geological surveys for permission to sample drillcores of the study units. Research by TJA was supported by grants from the National Science Foundation (EAR-0310072, EAR-0618003, and EAR-0745574) and the University of Cincinnati Research Council.

References

Algeo, T.J., Heckel, P.H., 2008. The Late Pennsylvanian Midcontinent Sea of North America: a review. Palaeogeogr. Palaeoclimatol. Palaeoecol. 268, 205–221.

Algeo, T.J., Lyons, T.W., 2006. Mo-total organic carbon covariation in modern anoxic marine environments: implication for analysis of paleoredox and -hydrographic conditions. Paleoceanography 21, PA1016 23 pp.

Algeo, T.J., Maynard, J.B., 2004. Trace-element behavior and redox facies in core shales of Upper Pennsylvanian Kansas-type cyclothems. Chem. Geol. 206, 289–318.

Algeo, T.J., Maynard, J.B., 2008. Trace metal covariation as a guide to water-mass conditions in ancient anoxic marine environments. Geosphere 4 (5), 872–887.

Algeo, T.J., Schwark, L., Hower, J.C., 2004. High-resolution geochemistry and sequence stratigraphy of the Hushpuckney Shale (Swope Formation, eastern Kansas): implications for climato-environmental dynamics of the Late Pennsylvanian Midcontinent Seaway. Chem. Geol. 206, 259–288.

Algeo, T.J., Lyons, W.L., Blakey, R.C., Over, D.J., 2007. Hydrographic conditions of the Devono-Carboniferous North American Seaway inferred from sedimentary Mo–TOC relationships. Palaeogeogr. Palaeoclimatol. Palaeoecol. 256, 204–230.

Algeo, T.J., Heckel, P.H., Maynard, J.B., Blakey, R., Rowe, H., 2008. Modern and ancient epicratonic seas and the superestuarine circulation model of marine anoxia. In: Holmden, C., Pratt, B.R. (Eds.), Dynamics of Epeiric Seas: Sedimentological, Paleontological and Geochemical Perspectives: Geol. Assoc. Canada Spec. Publ., vol. 48, pp. 7–38.

Anderson, R.F., 1987. Redox behavior of uranium in an anoxic marine basin. Uranium 3, 145–164.

Anderson, R.F., Fleischer, M.Q., 1991. Uranium precipitation in Black Sea sediments. In: Izdar, E., Murray, J.W. (Eds.), Black Sea Oceanography. Kluwer, Dordrecht, pp. 443–458.

Anderson, R.F., Fleischer, M.Q., LeHuray, A.P., 1989. Concentration, oxydation state and particle flux of Uranium in the Black Sea. Geochim. Cosmochim. Acta 53, 2215–2224.

Anderson, R.F., Lyons, T.W., Cowie, G.L., 1994. Sedimentary record of a shoaling of the oxic/anoxic interface in the Black Sea. Mar. Geol. 116, 373–384.

Arbenz, J.K., 1989. The Ouachita System. In: Bally, A.W., Palmer, A.R. (Eds.), The Geology of North America—An Overview. The Geology of North America, vol. A. Geol. Soc. Am, pp. 371–396.

Armstrong, D.K., 1986. Trace element geochemistry and petrology of the Kettle Point Formation (Upper Devonian), a black shale unit of southwestern Ontario. M.S. thesis, Univ. of Waterloo, Waterloo, Ontario, Canada, 234 pp.

Arthur, M.A., Dean, W.E., Neff, E.D., Hay, B.J., King, J., Jones, G., 1994. Varve-calibrated records of carbonate and organic carbon accumulation over the last 2000 years in the Black Sea. Glob. Biogeochem. Cycles 8, 195–217.

Astor, Y., Müller-Karger, F., Scranton, M.I., 2003. Seasonal and interannual variation in the hydrography of the Cariaco Basin: implications for basin ventilation. Cont. Shelf Res. 23, 125–144.

Barnes, C.E., Cochran, J.K., 1990. Uranium removal in oceanic sediments and the oceanic U balance. Earth Planet. Sci. Lett. 97, 94–101.

Barnes, C.E., Cochran, J.K., 1991. Geochemistry of uranium in Black Sea sediments. Deep-Sea Res. I 38 (suppl. 2A), S1237–S1254.

Berelson, W.M., 1991. The flushing of two deep-sea basins, southern California borderland. Limnol. Oceanogr. 36, 1150–1166.

Berelson, W.M., Hammond, D.E., Johnson, K.S., 1987. Benthic fluxes and cycling of biogenic silica and carbon in two southern California borderland basins. Geochim. Cosmochim. Acta 51, 1345–1363.

Berelson, W.M., McManus, J., Kilgore, T.E., Coale, K., Johnson, K., Burdige, D., Pilskaln, C., 1996. Biogenic matter diagenesis on the sea floor: a comparison between two continental margin transects. J. Mar. Res. 54, 731–762.

Berelson, W.M., Prokopenko, M., Sansone, F.J., Graham, A., McManus, J., Bernhard, J.M., 2005. Anaerobic diagenesis of silica and carbon in continental margin sediments: discrete zones of TCO_2 production. Geochim. Cosmochim. Acta 69, 4611–4629.

Berrang, P.G., Grill, E.V., 1974. The effect of manganese oxide scavenging on molybdenum in Saanich Inlet, British Columbia. Mar. Chem. 2, 125–148.

Bond, G.C., Kominz, M.A., 1991. Disentangling middle Paleozoic sea level and tectonic events in cratonic margins and cratonic basins of North America. J. Geophys. Res. 96, 6619–6639.

Böning, P., Brumsack, H.-J., Böttcher, M.E., Schnetger, B., Kriete, C., Kallmeyer, J., Borchers, S.L., 2004. Geochemistry of Peruvian near-surface sediments. Geochim. Cosmoch. Acta 68, 4429–4451.

Bruland, K.W., 1983. Trace elements in sea-water. In: Riley, J.P., Chester, R. (Eds.), 2nd ed. Chemical Oceanography, vol. 8. Academic Press, New York, pp. 157–220.

Brumsack, H.-J., 1980. Geochemistry of Cretaceous black shales from the Atlantic Ocean (DSDP Legs 11, 14, 36 and 41). Chem. Geol. 31, 1–25.

Calvert, S.E., Pedersen, T.F., 1993. Geochemistry of Recent oxic and anoxic marine sediments: Implications for the geological record. Mar. Geol. 113, 67–88.

Calvert, S.E., Karlin, R.E., Toolin, L.J., Donahue, D.J., Southon, J.R., Vogel, J.S., 1991. Low organic carbon accumulation rates in Black Sea sediments. Nature 350, 692–695.

Chaillou, G., Anschutz, P., Lavaux, G., Schäfer, J., Blanc, G., 2002. The distribution of Mo, U, and Cd in relation to major redox species in muddy sediments of the Bay of Biscay. Mar. Chem. 80, 41–59.

Chaillou, G., Schäfer, J., Blanc, G., Anschutz, P., 2008. Mobility of Mo, U, As, and Sb within modern turbidites. Mar. Geol. 254, 171–179.

Chan, F., Barth, J.A., Lubchenco, J., Kirincich, A., Weeks, H., Peterson, W.T., Menge, B.A., 2008. Emergence of anoxia in the California Current Large Marine Ecosystem. Science 319, 920.

Chen, J.H., Edwards, R.L., Wasserburg, G.J., 1986. ^{238}U, ^{234}U and ^{232}Th in seawater. Earth Planet. Sci. Lett. 80, 241–251.

Colley, S., Thomson, J., 1985. Recurrent uranium relocations in distal turbidites emplaced in pelagic conditions. Geochim. Cosmochim. Acta 49, 2339–2348.

Crowley, T.J., Hyde, W.T., Short, D.A., 1989. Seasonal cycle variations on the supercontinent of Pangaea. Geology 17, 457–460.

Crusius, J., Calvert, S., Pedersen, T., Sage, D., 1996. Rhenium and molybdenium enrichments in sediments as indicators of oxic, suboxic, and sulfidic conditions of deposition. Earth Planet. Sci. Lett. 145, 65–78.

de Baar, H.J.W., German, C.R., Elderfield, H., van Gaans, P., 1988. Rare earth element distributions in anoxic waters of the Cariaco Trench. Geochim. Cosmochim. Acta 52, 1203–1219.

Dean, W.E., Gardner, J.V., Piper, D.Z., 1997. Inorganic geochemical indicators of glacial–interglacial changes in productivity and anoxia on the California continental margin. Geochim. Cosmochim. Acta 61, 4507–4518.

Dean, W.E., Piper, D.Z., Peterson, L.C., 1999. Molybdenum accumulation in Cariaco Basin sediment over the last 24 ky: a record of water-column anoxia and climate. Geology 27, 507–510.

Dean, W.E., Zheng, Y., Ortiz, J.D., van Geen, A., 2006. Sediment Cd and Mo accumulation in the oxygen-minimum zone off western Baja California linked to global climate over the past 52 kyr. Paleoceanography 21, PA4209.

Degens, E.T., Ross, D.A. (Eds.), 1974. The Black Sea—geology, chemistry, and biology: Am. Assoc. Petrol. Geol., Mem., vol. 20. American Association of Petroleum Geologists, Tulsa, Oklahoma, 633 pp.

Emerson, S.R., Huested, S.S., 1991. Ocean anoxia and the concentration of molybdenum and vanadium in seawater. Mar. Chem. 34, 177–196.

Erickson, B.E., Helz, G.R., 2000. Molybdenum (VI) speciation in sulfidic waters: stability and lability of thiomolybdates. Geochim. Cosmochim. Acta 64, 1149–1158.

Ettensohn, F.R., 1985. Controls on development of Catskill delta complex basin facies. In: Woodrow, D.L., Sevon, W.D. (Eds.), The Catskill Delta: Geol. Soc. Am. Spec. Paper, vol. 201, pp. 65–77.

Ettensohn, F.R., Barron, L.S., 1983. A tectonic–climatic approach to the deposition of the Devonian–Mississippian black-shale sequence of North America. Proceedings of the 1982 Eastern Oil Shale Symposium. Kentucky Department of Energy and University of Kentucky Institute for Mining and Mineral Resources, Lexington, Kentucky, pp. 5–37.

François, R., 1988. A study on the regulation of the concentrations of some trace metals (Rb, Sr, Zn, Pb, Cu, V, Cr, Ni, Mn and Mo) in Saanich Inlet sediments, British Columbia, Canada. Mar. Geol. 83, 285–308.

Frost, J.K., Zierath, D.L., Shimp, N.F., 1985. Chemical Composition and Geochemistry of the New Albany Shale Group (Devonian–Mississippian) in Illinois. Illinois State Geol. Surv. Contract Report 1985–4 (U.S. Dept of Energy contract DE-AC21-76ET12142), 134 pp.

Gardner, J.V., Hemphill-Haley, E., 1986. Evidence for a stronger oxygen-minimum zone off central California during late Pleistocene to early Holocene. Geology 14, 691–694.

Haq, B.U., Schutter, S.R., 2008. A chronology of Paleozoic sea-level changes. Science 322, 64–68.

Hartwell, W.J., 1998. Geochemical and petrographic analysis of the Upper Devonian–Lower Mississippian Bakken black shales from the Williston Basin, North Dakota. M.S. Thesis, Univ. of Cincinnati, Cincinnati, Ohio, 256 pp.

Haug, G.H., Pedersen, T.F., Sigman, D.M., Calvert, S.E., Nielsen, B., Peterson, L.C., 1998. Glacial/interglacial variations in production and nitrogen fixation in the Cariaco Basin during the last 580 kyr. Paleoceanography 13, 427–432.

Heckel, P.H., 1977. Origin of phosphatic black shale facies in Pennsylvanian cyclothems of mid-continent North America. Am. Assoc. Pet. Geol. Bull. 61, 1045–1068.

Helz, G.R., Miller, C.V., Charnock, J.M., Mosselmans, J.L.W., Pattrick, R.A.D., Garner, C.D., Vaughan, D.J., 1996. Mechanisms of molybdenum removal from the sea and its concentration in black shales: EXAFS evidences. Geochim. Cosmochim. Acta 60, 3631–3642.

Ho, T.-Y., Taylor, G.T., Astor, Y., Varela, M., Muller-Karger, F., Scranton, M.I., 2004. Vertical and temporal variability of redox zonation in the water column of the Cariaco Basin: implications for organic carbon oxidation pathways. Mar. Chem. 86, 89–104.

Hoffman, D.L., Algeo, T.J., Maynard, J.B., Joachimski, M.M., Hower, J.C., Jaminski, J., 1998. Regional and stratigraphic variation in bottom-water anoxia in offshore core shales of Upper Pennsylvanian cyclothems from the Eastern Mid-continent Shelf (Kansas), USA. In: Schieber, J., Zimmerle, W., Sethi, P.S. (Eds.), Shales and Mudstones, vol. 1. Schweizerbart, Stuttgart, pp. 243–269.

Holmden, C., Creaser, R.A., Muehlenbachs, K., Leslie, S.A., Bergström, S.M., 1998. Isotopic evidence for geochemical decoupling between ancient epeiric seas and bordering oceans: implications for secular curves. Geology 26, 567–570.

Howell, P.D., van der Pluijm, B.A., 1990. Early history of the Michigan Basin : subsidence and Appalachian tectonics. Geology 18, 1195–1198.

Howell, P.D., van der Pluijm, B.A., 1999. Structural sequences and styles of subsidence in the Michigan Basin. Geol. Soc. Am. Bull. 111, 974–991.

Hurtgen, M.T., Lyons, T.W., Ingall, E.D., Cruse, A.M., 1999. Anomalous enrichments of iron monosulfide in euxinic marine sediments and the role of H_2S in iron sulfide transformations: examples from Effingham Inlet, Orca Basin, and the Black Sea. Am. J. Sci. 299, 556–588.

Immenhauser, A., Holmden, C., Patterson, W.P., 2008. Interpreting the carbon-isotope record of ancient shallow epeiric seas: lessons from the Recent. In: Holmden, C., Pratt, B.R. (Eds.), Dynamics of epeiric seas: sedimentological, paleontological and geochemical perspectives: Geol. Assoc. Canada Spec. Publ., vol. 48, pp. 137–174.

Irino, T., Pedersen, T.F., et al., 2000. Geochemical character of glacial to interglacial sediments at Site 1017, Southern California margin; minor and trace elements. Proc. Ocean Drill. Program, Sci. Rep. 167, 263–271.

Jacobs, L.A., 1984. Metal geochemistry in anoxic marine basins. Ph.D. dissertation, Univ. Of Washington, Seattle, Washington, 217 pp.

Jacobs, L., Emerson, S., Skei, J., 1985. Partitioning and transport of metals across the O_2/H_2S interface in a permanently anoxic basin: Framvaren Fjord, Norway. Geochim. Cosmochim. Acta 49, 1433–1444.

Jacobs, L., Emerson, S., Huested, S.S., 1987. Trace metal geochemistry in the Cariaco Trench. Deep-Sea Res. I 34, 965–981.

Jaminski, J., 1997. Geochemical and petrographic patterns of cyclicity in the Devonian–Mississippian black shales of the Central Appalachian Basin. Ph.D. dissertation, Univ. of Cincinnati, Cincinnati, Ohio, 333 pp.

Jaminski, J., Algeo, T.J., Maynard, J.B., Hower, J.C., 1998. Climatic origin of dm-scale compositional cyclicity in the Cleveland Member of the Ohio Shale (Upper Devonian), Central Appalachian Basin, USA. In: Schieber, J., Zimmerle, W., Sethi, P.S. (Eds.), Shales and Mudstones, vol. 1. Schweizerbart'sche, Stuttgart, pp. 217–242.

Johnson, J.G., Klapper, G., Sandberg, C.A., 1985. Devonian eustatic fluctuations in Euramerica. Geol. Soc. Am. Bull. 96, 567–587.

Karl, D.M., Knauer, G.A., 1991. Microbial production and particle flux in the upper 350 m of the Black Sea. Deep-Sea Res. I 38, S921–S942.

Karma, R., 1991. Geology and geochemistry of the Bakken Formation (Devonian–Mississippian) in Saskatchewan. M.S. thesis, Univ. of Regina, Regina, Saskatchewan, Canada, 308 pp.

Kennett, J.P., Ingram, B.L., 1995. A 20, 000 year record of ocean circulation and climate change from the Santa Barbara basin. Nature 377, 510–513.

Kennett, J.P., Roark, E.B., Cannariato, K.G., Ingram, B.L., Tada, R., 2000. Latest Quaternary paleoclimatic and radiocarbon chronology, ODP Hole 1017E, southern California margin. Proc. Ocean Drill. Program, Sci. Rep. 167, 249–254.

Klinkhammer, G.P., Palmer, M.R., 1991. Uranium in the oceans: where it goes and why. Geochim. Cosmochim. Acta 55, 1799–1806.

Langmuir, D., 1978. Uranium solution-mineral equilibria at low temperatures with applications to sedimentary ore deposits. Geochim. Cosmochim. Acta 42, 547–569.

Leventhal, J.S., Hosterman, J.W., 1982. Chemical and mineralogical analysis of Devonian black-shale samples from Martin County, Kentucky; Carroll and Washington counties, Ohio, Wise County, Virginia; and Overton County, Tennessee, U.S.A. Chem. Geol. 37, 239–264.

Levitus, S., Boyer, T., 1994. World Ocean Atlas 1994, vol. 2: Oxygen. NOAA Atlas NESDIS 2, U.S. Dept. of Commerce, Washington, D.C. (iridl.ldeo.columbia.edu/sources/.levitus94/.annual/.O2/).

Lyons, T.W., 1992. Comparative study of Holocene Black Sea sediments from oxic and anoxic sites of deposition: geochemical and sedimentological criteria, Ph.D. dissertation, Yale University, New Haven, Connecticut, 377 pp.

Lyons, T.W., Berner, R.A., Anderson, R.F., 1993. Evidence for large pre-industrial perturbations of the Black Sea chemocline. Nature 365, 538–540.

Lyons, T.W., Werne, J.P., Hollander, D.J., Murray, R.W., 2003. Contrasting sulfur geochemistry and Fe/Al and Mo/Al ratios across the last oxic-to-anoxic transition in the Cariaco Basin, Venezuela. Chem. Geol. 195, 131–157.

Magyar, B., Moor, H.C., Sigg, L., 1993. Vertical distribution and transport of molybdenum in a lake with a seasonally anoxic hypolimnion. Limnol. Oceanogr. 38, 521–531.

McManus, J., Berelson, W.M., Klinkhammer, G.P., Hammond, D.E., Holm, C., 2005. Authigenic uranium: relationship to oxygen penetration depth and organic carbon rain. Geochim. Cosmochim. Acta 69, 95–108.

McManus, J., Berelson, W.B., Severmann, S., Poulson, R.L., Hammond, D.E., Klinkhammer, G.P., Holm, C., 2006. Molybdenum and uranium geochemistry in continental margin sediments: paleoproxy potential. Geochim. Cosmochim. Acta 70, 4643–4662.

Meyers, S.R., Sageman, B.B., Lyons, T.W., 2005. Organic carbon burial rate and the molybdenum proxy: theoretical framework and application to Cenomanian–Turonian oceanic event 2. Paleoceanography, 20, p. PA2002. 19 pp.

Millero, F.J., 1996. Chemical Oceanography. CRC Press, Boca Raton, Florida. 469 pp.

Montañez, I.P., Tabor, N.J., Niemeier, D., DiMichele, W.A., Frank, T.D., Fielding, C.R., Isbell, J.L., Birgenheier, L.P., Rygel, M.C., 2007. CO_2-forced climate and vegetation instability during Late Paleozoic deglaciation. Science 315, 87–91.

Morford, J.L., Emerson, S., 1999. The geochemistry of redox sensitive trace metals in sediments. Geochim. Cosmochim. Acta 63, 1735–1750.

Morford, J.L., Emerson, S.R., Breckel, E.J., Kim, S.H., 2005. Diagenesis of oxyanions (V, U, Re, and Mo) in pore waters and sediments from a continental margin. Geochim. Cosmochim. Acta 69, 5021–5032.

Morford, J.L., Martin, W.R., Carney, C.M., 2009a. Uranium diagenesis in sediments underlying bottom waters with high oxygen content. Geochim. Cosmochim. Acta 73, 2920–2937.

Morford, J.L., Martin, W.R., François, R., Carney, C.M., 2009b. A model for uranium, rhenium, and molybdenum diagenesis in marine sediments based on results from coastal locations. Geochim. Cosmochim. Acta 73, 2938–2960.

Morris, A.W., 1975. Dissolved molybdenum and vanadium in the northeast Atlantic Ocean. Deep-Sea Res. 22, 49–54.

Müller-Karger, F., Varela, R., Thunell, R., Scranton, M.I., Bohrer, R., Taylor, G.T., Capelo, J., Astor, Y., Tappa, E., Ho, T.-Y., Walsh, J.J., 2001. The annual cycle of primary production in the Cariaco Basin: response to upwelling and implications for vertical export. J. Geophys. Res. 106, 4527–4542.

Murray, J.W., 1975. The interaction of metal ions at the manganese dioxide-solution interface. Geochim. Cosmochim. Acta 42, 1011–1026.

Murray, J.W., Jannasch, H.W., Honjo, S., Anderson, R.F., Reeburgh, W.S., Top, Z., Friederich, G.E., Codispoti, L.A., Izdar, E., 1989. Unexpected changes in the oxic/anoxic interface in the Black Sea. Nature 338, 411–413.

Murray, J.W., Top, Z., Özsoy, E., 1991. Hydrographic properties and ventilation of the Black Sea. Deep-Sea Res. I 38 (suppl. 2), S663–S689.

Nameroff, T.J., Balistrieri, L.S., Murray, J.W., 2002. Suboxic trace metal geochemistry in the eastern tropical North Pacific. Geochim. Cosmochim. Acta 66, 1139–1158.

Panchuk, K.M., Holmden, C., Kump, L.R., 2005. Sensitivity of the epeiric sea carbon isotope record to local-scale carbon cycle processes: tales from the Mohawkian Sea. Palaeogeogr. Palaeoclimatol. Palaeoecol. 228, 320–337.

Parrish, J.T., 1993. Climate of the supercontinent Pangea. J. Geol. 101, 215–233.

Perkins, R.B., Piper, D.Z., Mason, C.E., 2008. Trace-element budgets in the Ohio/Sunbury shales of Kentucky: constraints on ocean circulation and primary productivity in the Devonian–Mississippian Appalachian Basin. Palaeogeogr. Palaeoclimatol. Palaeoecol. 265, 14–29.

Peterson, L.C., Overpeck, J.T., Kipp, N.G., Imbrie, J., 1991. A high-resolution Late Quaternary upwelling record from the anoxic Cariaco Basin, Venezuela. Paleoceanography 6, 99–119.

Potter, P.E., Maynard, J.B., Pryor, W.A., 1982. Appalachian gasbearing Devonian shales: statements and discussion. Oil Gas J. 80, 290–318.

Poulsen, C.J., Pollard, D., Montanez, I.P., Rowley, D., 2007. Late Paleozoic tropical climate response to Gondwanan deglaciation. Geology 35, 771–774.

Poulson, R.L., Siebert, C., McManus, J., Bereleson, W.M., 2006. Authigenic molybdenum isotope signatures in marine sediments. Geology 34, 617–620.

Presley, B.J., Stearns, S., 1986. Interstitial water chemistry, Deep Sea Drilling Project Leg 961. In: Bouma, A.H., Coleman, J.M., Meyer, A.W., et al. (Eds.), Init. Repts. Deep Sea Drilling Proj., vol. 96. Govt. Printing Office, Washington, D.C, pp. 697–709.

Reimers, C.E., Suess, E., 1983. Spatial and temporal patterns of organic matter accumulation on the Peru continental margin. In: Suess, E., Thiede, J. (Eds.), Coastal upwelling, its sediment record. Part B. Plenum, New York, pp. 311–345.

Rheams, K.F., Neathery, T.L., 1988. Characterization and geochemistry of Devonian oil shale, North Alabama, Northwest Georgia, and South-Central Tennessee (a resource evaluation). Alabama Geol. Surv. Bull., vol. 128. 214 pp.

Rimmer, S.M., 2004. Geochemical paleoredox indicators in Devonian–Mississippian black shales, Central Appalachian Basin (USA). Chem. Geol. 206, 373–391.

Sageman, B.B., Murphy, A.E., Werne, J.P., Ver Straeten, C.A., Hollander, D.J., Lyons, T.W., 2003. A tale of shales: the relative roles of production, decomposition, and dilution in the accumulation of organic-rich strata, Middle–Upper Devonian, Appalachian basin. Chem. Geol. 195, 229–273.

Savrda, C.E., Bottjer, D.J., 1991. Oxygen-related biofacies in marine strata: an overview and update. In: Tyson, R.V., Pearson, T.H. (Eds.), Modern and ancient continental shelf anoxia: Geol. Soc. London Spec. Publ., vol. 58, pp. 201–219.

Schieber, J., 1994a. Evidence for high-energy events and shallow-water deposition in the Chattanooga Shale, Devonian, central Tennessee, USA. Sediment. Geol. 93, 193–208.

Schieber, J., 1994b. Reflection of deep vs. shallow water deposition by small-scale sedimentary features and microfabrics of the Chattanooga Shale in Tennessee. In: Embry, A.F., Beauchamp, B., Glass, D.J. (Eds.), Pangea: global environments and resources: Canad. Soc. Petrol. Geol. Mem., vol. 17, pp. 773–784.

Schieber, J., 1994c. Paleoflow patterns and macroscopic sedimentary features in the Late Devonian Chattanooga Shale of Tennessee; differences between the western and eastern Appalachian Basin. In: Embry, A.F., Beauchamp, B., Glass, D.J. (Eds.), Pangea : global environments and resources: Canad. Soc. Petrol. Geol. Mem., vol. 17, pp. 763–772.

Schieber, J., 1998a. Sedimentary features indicating erosion, condensation, and hiatuses in the Chattanooga Shale of central Tennessee: relevance for sedimentary and stratigraphic evolution. In: Schieber, J., Zimmerle, W., Sethi, P.S. (Eds.), Shales and Mudstones, vol. 1. Schweizerbart'sche, Stuttgart, pp. 187–215.

Schieber, J., 1998b. Developing a sequence stratigraphic framework for the Late Devonian Chattanooga Shale of the Southeastern U.S.A.: relevance for the Bakken Shale. Eighth International Williston Basin Symposium. Saskatchewan Geol. Soc., Regina, pp. 58–68.

Schieber, J., Riciputi, L., 2004. Pyrite ooids in Devonian black shales record intermittent sea-level drop and shallow-water conditions. Geology 32, 305–308.

Scranton, M.I., Sayles, F.L., Bacon, M.P., Brewer, P.G., 1987. Temporal changes in the hydrography and chemistry of the Cariaco Trench. Deep-Sea Res. I 34, 945–963.

Scranton, M.I., Astor, Y., Bohrer, R., Ho, T.-Y., Müller-Karger, F., 2001. Controls on temporal variability of the geochemistry of the deep Cariaco Basin. Deep-Sea Res. I 48, 1605–1625.

Shaw, T.J., Gieskes, J.M., Jahnke, R.J., 1990. Early diagenesis in differing depositional environments: the response of transition metals in pore water. Geochim. Cosmochim. Acta 54, 1233–1246.

Sheu, D.-D., 1990. The anoxic Orca Basin (Gulf of Mexico): geochemistry of brines and sediments. Rev. Aquat. Sci. 2, 491–507.

Sheu, D.-D., Shakur, A., Pigott, J.D., Wiesenburg, D.A., Brooks, J.M., Krouse, H.R., 1987. Sulfur and oxygen isotopic compositions of dissolved sulfate in the Orca Basin: implications for origin of the high-salinity brine and oxidation of sulfides at the brine–seawater interface. Mar. Geol. 78, 303–310.

Shokes, R.F., Trabant, P.K., Presley, B.J., Reid, D.R., 1977. Anoxic, hypersaline basin in the northern Gulf of Mexico. Science 196, 1443–1446.

Skei, J., Loring, D.H., Rantala, R.T.T., 1996. Trace metals in suspended particulate matter and in sediment trap material from a permanently anoxic fjord—Framvaren, south Norway. Aquat. Geochem. 2, 131–147.

Suits, N.S., Arthur, M.A., 2000. Bacterial production of anomalously high dissolved sulfate concentrations in Peru slope sediments: steady-state sulfur oxidation, or transient response to end of El Niño? Deep-Sea Res. I 47, 1829–1853.

Tada, R., et al., 2000. Millennial-scale compositional variations in late Quaternary sediments at Site 1017, Southern California. In: Miller, C.M., Nessler, S., Peters, L.L. (Eds.), Proc. Ocean Drilling Prog., Sci. Repts., vol. 167, pp. 277–296.

Taylor, S.R., McLennan, S.M., 1985. The continental crust: its composition and evolution. Blackwell, Oxford. 312 pp.

Taylor, G.T., Iabichella, M., Ho, T.-Y., Scranton, M.I., Thunell, R.C., Varela, R., 2001. Chemoautotrophy in the redox transition zone of the Cariaco Basin: a significant source of midwater organic carbon production. Limnol. Oceanogr. 46, 148–163.

Thomson, J., Higgs, N.C., Wilson, T.R.S., Croudace, L.W., de Lange, G.J., van Santvoort, P.J.M., 1995. Redistribution and geochemical behavior of redox-sensitive elements around S1, the most recent eastern Mediterranean sapropel. Geochim. Cosmochim. Acta 59, 3487–3501.

Thomson, J., Jarvis, I., Green, D.R.H., Green, D., 1998. Oxidation fronts in Madeira Abyssal Plain turbidites: persistence of early diagenetic trace-element enrichments during burial, Site 950. In: Weaver, P.P.E., Schmincke, H.-U., Firth, J.V., Duffield, W. (Eds.), Proc. Ocean Drilling Prog., Sci. Repts., vol. 157, pp. 559–572.

Thunell, R.C., Tappa, E., Anderson, D.M., 1995. Sediment fluxes and varve formation in Santa Barbara Basin. Geology 23, 1083–1086.

Thunell, R.C., Varela, R., Llano, M., Collister, J., Muller-Karger, F., Bohrer, R., 2000. Organic carbon fluxes, degradation, and accumulation in an anoxic basin: sediment trap results from the Cariaco Basin. Limnol. Oceanogr. 45, 300–308.

Trefry, J.H., Presley, B.J., Keeney-Kennicutt, W.L., Trocine, R.P., 1984. Distribution and chemistry of manganese, iron, and suspended particulates in Orca Basin. Geo-Mar. Lett. 4, 125–130.

Tribovillard, N., Riboulleau, A., Lyons, T., Baudin, F., 2004. Enhanced trapping of molybdenum by sulfurized organic matter of marine origin as recorded by various Mesozoic formations. Chem. Geol. 213, 385–401.

Tribovillard, N., Algeo, T., Lyons, T.W., Riboulleau, A., 2006. Trace metals as paleoredox and paleoproductivity proxies: an update. Chem. Geol. 232, 12–32.

Tribovillard, N., Bout-Roumazeilles, V., Algeo, T., Lyons, T.W., Sionneau, T., Montero-Serrano, J.C., Riboulleau, A., Baudin, F., 2008. Paleodepositional conditions in the Orca Basin as inferred from organic matter and trace metal contents. Mar. Geol. 254, 62–72.

Tugrul, S., Basturk, O., Saydam, C., Yilmaz, A., 1992. Changes in the hydrochemistry of the Black Sea inferred from water density profiles. Nature 359, 137–139.

Van Cappellen, P., Viollier, E., Roychoudhury, A., Clark, L., Ingall, E., Lowe, K., DiChristina, T., 1998. Biogeochemical cycles of manganese and iron at the oxic–anoxic transition of a stratified marine basin (Orca Basin, Gulf of Mexico). Environ. Sci. Technol. 32, 2931–2939.

Van der Weijden, C.H., 2002. Pitfalls of normalization of marine geochemical data using a common divisor. Mar. Geol. 184, 167–187.

Van Geen, A., Zheng, Y., Berhard, J.M., Cannariato, K.G., Carriquiry, J., Dean, W.E., Eakins, B.W., Ortiz, J.D., Pike, J., 2003. On the preservation of laminated sediments along the western margin of North America. Paleoceanography 18 (4) 1098, 17 pp.

Vorlicek, T.P., Helz, G.R., 2002. Catalysis by mineral surfaces: implications for Mo geochemistry in anoxic environments. Geochim. Cosmochim. Acta 66, 3679–3692.

Werne, J.P., Hollander, D.J., Lyons, T.W., Peterson, L.C., 2000. Climate-induced variations in productivity and planktonic ecosystem structure from the Younger Dryas to Holocene in the Cariaco Basin, Venezuela. Paleoceanography 15 (1), 19–29.

Werne, J.P., Hollander, D.J., Lyons, T.W., Sageman, B.B., 2002. An integrated assessment of a "type euxinic" deposit; evidence for multiple controls on black shale deposition in the Middle Devonian Oatka Creek Formation. Am. J. Sci. 302, 110–143.

Wignall, P.B., 1994. Black Shales. Clarendon Press, Oxford. 127 pp.

Wignall, P.B., Myers, K.J., 1988. Interpreting benthic oxygen levels in mudrocks: a new approach. Geology 16, 452–455.

Wilkin, R.T., Arthur, M.A., 2001. Variations in pyrite texture, sulfur isotope composition, and iron systematics in the Black Sea; evidence for late Pleistocene to Holocene excursions of the O_2–H_2S redox transition. Geochim. Cosmochim. Acta 65, 1399–1416.

Woodrow, D.L., 1985. Paleogeography, paleoclimate, and sedimentary processes of the Late Devonian Catskill Delta. In: Woodrow, D.L., Sevon, W.D. (Eds.), The Catskill Delta: Geol. Soc. Am. Spec. Pap., vol. 201, pp. 51–63.

Wyrtki, K., 1967. Circulation and water masses in the eastern equatorial Pacific Ocean. Int. J. Oceanogr. Limnol. 1, 117–147.

Zhang, J.-Z., Millero, J.J., 1993. The chemistry of anoxic waters in the Cariaco Trench. Deep-Sea Res. I 40, 1023–1041.

Zheng, Y., Anderson, R.F., van Geen, A., Kuwabara, J., 2000. Authigenic molybdenium formation in marine sediments: a link to pore water sulfide in the Santa Barbara Basin. Geochim. Cosmochim. Acta 64, 4165–4178.

Zheng, Y., Anderson, R.F., van Geen, A., Fleischer, M.Q., 2002a. Preservation of non-lithogenic particulate uranium in marine sediments. Geochim. Cosmochim. Acta 66, 3085–3092.

Zheng, Y., Anderson, R.F., van Geen, A., Fleischer, M.Q., 2002b. Remobilization of authigenic uranium in marine sediments by bioturbation. Geochim. Cosmochim. Acta 66, 1759–1772.

Zoback, M.D., Zoback, M.L., 1991. Tectonic stress field of North America and relative plate motions. In: Engdahl, E.R., Zoback, M.D., Blackwell, D.D. (Eds.), Neotectonics of North America, Geol. Soc. Am., Geology of North America, vol. Suppl. 1, pp. 339–366.

Zuta, S., Guillén, O., 1970. Oceanografia de las aguas costeras del Peru. Inst. Mar. Peru Boll. 2, 161–323.

Zuta, S., Rivera, T., Bustamante, A., 1978. Hydrologic aspects of the main upwelling areas off Peru. In: Boje, R., Tomczak, M. (Eds.), Upwelling Ecosystems. Springer, Berlin, pp. 235–257.